ONLINE DIVERSION DETECTION IN CYCLUS

BY

GREG T. WESTPHAL

THESIS

Submitted in partial fulfillment of the requirements
for the degree of Master of Science in Nuclear, Plasma, and Radiological Engineering
in the Graduate College of the
University of Illinois at Urbana-Champaign, 2019

Urbana, Illinois

Master's Committee:

        Assistant Professor Kathryn Huff, Chair
        Unknown Professor

Abstract

Abstract

dedication

Table of Contents

Chapter 1

Introduction

The diversion of significant quantities of Special Nuclear Material (SNM) from the nuclear fuel cycle is a major non-proliferation concern [1]. These diversions must be detected in a timely manner using signatures and observables in order to properly safeguard the fuel cycle. Timely detection is critical in non-proliferation to discover these shadow fuel cycles before diverted material is further processed. Pyroprocessing is a used nuclear fuel separations technology for advanced reactors. Signatures and observables are used to detect diversion of nuclear material. The goal of this research is to identify potential signs of material diversion in a pyroprocessing facility and implement models of these processes into a detailed pyroprocessing facility archetype to the modular, agent-based fuel cycle simulator, CYCLUS [2]. This facility archetype will equip users of the CYCLUS fuel cycle simulator to investigate detection timeliness enabled by measuring signatures and observables in various fuel cycle scenarios.

1.1 Motivation

1.1.1 Safeguards

Currently there are no commercially operated pyroprocessing plants, however various research designs exist in national labs, notably Argonne National Lab (ANL), Idaho National Lab (INL) and in South Korea, KAERI [3, 4, 5]. Therefore, prior to construction of any design we want to implement safeguards by design. Similar to security by design in next

generation reactors, the goal is to include key measurement points and access points to the design of the facility. Rather than learn from mistakes, in the future we aim to incorporate safety into the design.

1.1.2 Pyroprocessing

For other fuel cycle facilities, we have plenty of operating experience to inform on safeguard construction. For example, with aqueous reprocessing the International Atomic Energy Agency (IAEA) provides detailed flow-sheets of example facilities [6]. Multiple modeling tools have been developed for electrochemical processes such as SSPM and AMPYRE to combat this lack of operational experience for pyroprocessing plants [31]. These tools take a high fidelity approach to model the chemistry taking place within each chamber. In order to run these tools, the user must have intimate knowledge of the specific facility the flowsheets have been designed for. There is a gap, however, in the medium fidelity models that can inform on broader fuel cycle applications. A generic facility capable of modeling changes in operational settings and various layouts has not yet been implemented to a fuel cycle simulator [7].

1.1.3 Future Fuel Cycles

As the world begins to consider cleaner forms of energy in response to climate change, nuclear energy has regained traction. A main concern with nuclear power is the pileup of used nuclear fuel (UNF) as a result of the once-through fuel cycle. One suggested solution is converting to a closed fuel cycle [8]. There are many approaches to transitioning from our current fuel cycle to a new or closed cycle. Of these evaluation groups (EGs), those involving sodium fast reactors (SFRs) are of interest. Pyroprocessing can transition between current fuel cycle scenarios with light water reactors (LWRs) and SFRs and other metallic fuel. Therefore, pyroprocessing is under consideration as a means of processing the fuel required

to start up new breeder reactors for the EG01-EG24 transition scenario.

1.2 Background

1.2.1 Pyroprocessing

Pyroprocessing is an electrochemical separation method used primarily for metallic fast reactor fuel. This reprocessing technique uses molten salt, which differs depending on the facility, to provide a medium for current to travel across. Molten salt such as LiCl-KCl has a broader stability range compared to water, allowing high potentials to be used for separation. Traditionally, separation would be conducted in a nitric acid which uses water as its medium. This becomes a problem when considering heavier elements such as lanthanides and actinides. Controlling the oxidation states of these elements often requires potentials outside the stability of water. Hence, pyroprocessing was born to improve non-proliferation and reprocessing capabilities.

In addition to the improved redox control of heavier elements, we co-extract materials of interest so they cannot easily be refined for weapons. This is done through the electrorefining and electrowinning stages by separating a pure uranium stream as well as a uranium/transuranic (U/TRU) mix stream. The U/TRU can then be readily used for fuel fabrication while maintaining proliferation resistance.

Electrochemical Separations

Electrochemical separation is the driving force behind pyroprocessing. Electrochemistry relies on the use of Gibbs free energy to determine the required amount of energy to drive a reaction forward.

Figure 1.1 demonstrates an electrochemical process that generates electricity as a basic example. The processes described here follow the same principles but requires energy to
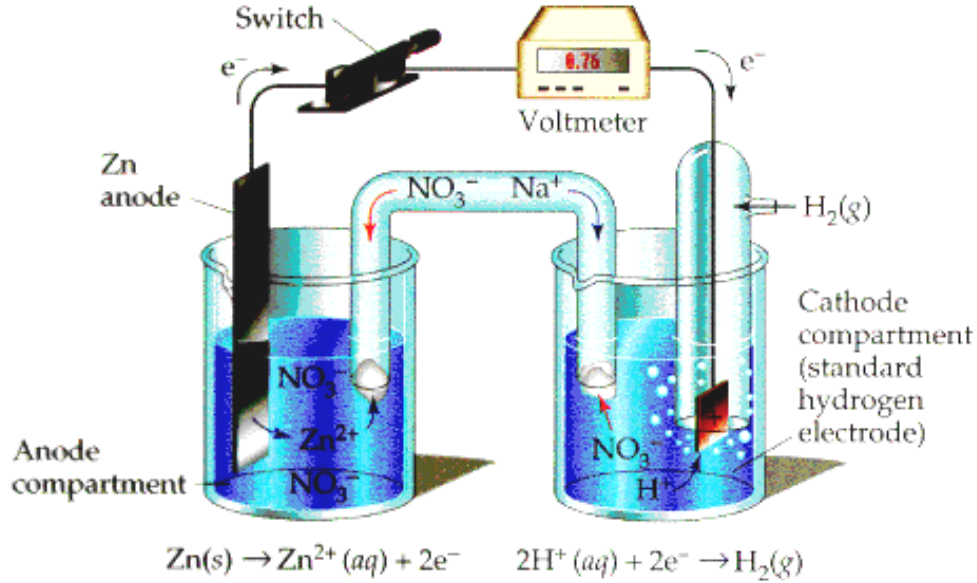
Figure 1.1: Basic example of movement of ions within a galvanic cell [9].

run. As shown in this basic example, ions are exchanged between the anode and cathode in an attempt to balance the potential difference. In the case of pyroprocessing, the potential difference is artificially applied. A number of different anodes and cathodes are used to force the desired ions to deliver charge from one end of the cell to the other. These ions that collect on the surface of the cathode can then be removed from the liquid and separated from the rest of the solution. By controlling the voltage of the solution as well as the composition of the anode, cathode, and electrolyte we can ensure the removal of unwanted elements/isotopes.

Voloxidation

Voloxidation is used following the chopping and decladding of the spent fuel. The process is very similar to annealing in regards to materials. The uranium dioxide is heated to temperatures around 700-1000°C which allows gases and some fission products to escape the fuel pellet, as well as convert UO_2 to U_3O_8 [10]. Voloxidation, in most cases, takes place in air which provides plenty of oxygen for oxidization of solid UO_2 [11]:

4

$$3UO_2 + O_2 \rightarrow U_3O_8$$
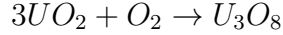
The above reaction is possible because of the expansion of uranium at elevated temperatures. A positive feedback is also established; as the uranium dioxide converts to yellowcake powder, the fuel element expands, exposing more uranium dioxide to oxygen. The rate of this reaction/conversion is dependent on the temperature and gas used. Higher temperatures will yield a faster reaction rate; even 500 $°C$ is sufficient for 99% reduction in 4 hours.

An added benefit of running a pyroprocessing voloxidation sub-process at the temperatures previously mentioned, 700-1000$°C$, is the removal of some fission products. The PRIDE facility at KAERI takes it a step further and voloxidates at 1250$°C$ to remove troublesome fission products at the beginning of the cycle[10]:

Voloxidation temperature	H-3	C-14	Kr-85	I-129	Cs	Tc	Ru	Rh	Te	Mo
1 250ºC	100	100	100	100	98	100	100	80	90	80

Figure 1.2: Voloxidation separation stream composition at 1250 $°C$

As shown in the table above, a majority of high activity isotopes are removed from the system at the beginning of pyroprocessing, protecting equipment and workers down the line. These gases are sent to an off-gas treatment facility that makes use of various scrubbing techniques such as liquid scrubbing, cyrogenic distillation (for the krypton), caustic scrubbing, etc [11].

Electroreduction

Following off-gassing and conversion to yellowcake, the non-metallic fuel must be converted and reduced to a molten salt mixture. In most cases this is done with a LiCl-KCl salt eutectic combined with Li_2O catalyst. The electrolytic reduction phase consists of three main parts: UO_2 recovery, reduction, and rare earth (RE) removal.
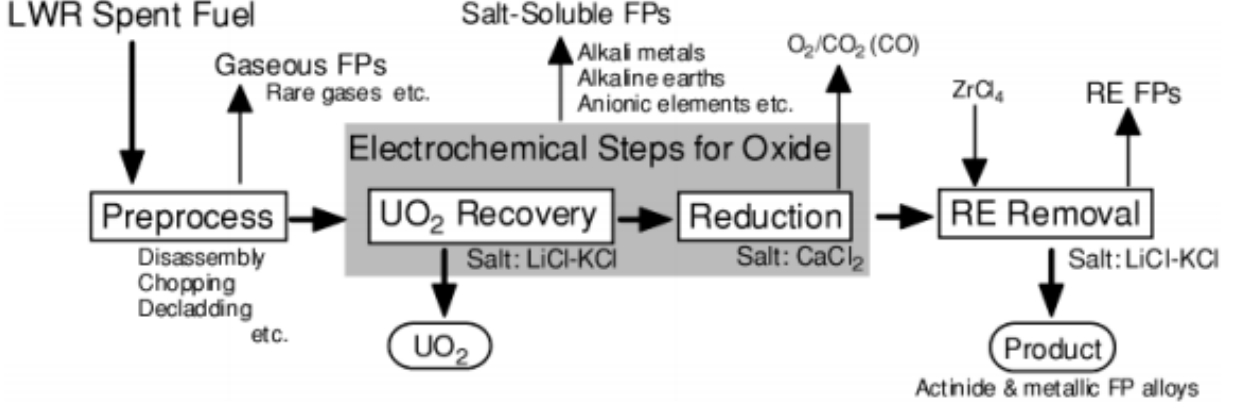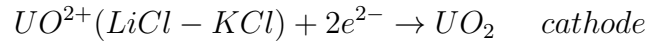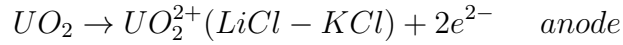
Figure 1.3: Electroreduction flow sheet [12].

The first step in electrolytic reduction is the recovery of UO_2 before reducing the remaining material. The following equations dictate the transfer of uranium from the anode to cathode.

$$UO_2 \rightarrow UO_2^{2+}(LiCl - KCl) + 2e^{2-} \quad anode$$

$$UO^{2+}(LiCl - KCl) + 2e^{2-} \rightarrow UO_2 \quad cathode$$

As in other separations technologies, noble metals can often follow the uranium through the rest of the process. The lurking noble metal fission products (FPs) cause an increase in radioactivity of the UO_2 stream. Therefore, the weight percent dissolution of uranium is critical in reducing the amount of waste that follows to the product stream. Lithium oxide can also be used as a catalyst to draw uranium to the cathode while leaving the noble metal fission products in the salt. This is done with 1-3wt% Li_2O in the following equations [13]:

$$Li_2O \rightarrow 2Li^+ + O^{2-}$$

$$UO_{x/2} + xLi \rightarrow U + xLi_2O$$
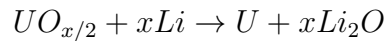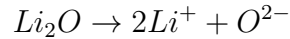
These equations make a continuously driven loop dragging uranium (either UO_2 or U_3O_8) from the anode to the cathode. Disproportionated lithium ions from the first equation break

6

apart the uranium and oxide, with help from the electric potential. The U collects on the cathode while the Li_2O is recycled and drives the first equation forward again. Reduction then occurs on the cathode where the U, TRU, REs, and noble metals (NMs) have collected. This is achieved by evolving oxygen gas along the anode using the following reactions[13, 10]:

$$Li^+ \rightarrow Li + e^- \qquad Cathode$$

$$M_xO_y + 2yLi \rightarrow xM + yLi_2O \qquad Cathode$$

$$O^{2-} \rightarrow 0.5O_2 + 2e^- \qquad Anode$$
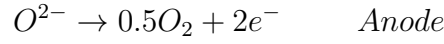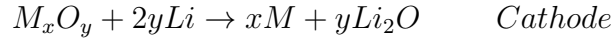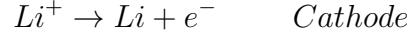
Electrochemical reduction results in an alloy of reduced U/TRU/RE/NM; however, we want to minimize the amount of RE and NM in the product. We've touched already on how to reduce the quantity of NM and for the final step the RE must be removed. The RE FPs can be removed from the alloy by substituting another chloride into the LiCl-KCl eutectic. In the case of Ohta et al. $ZrCl_4$ was considered [12]:

$$3ZrCl_4(LiCl - KCl) + RE \rightarrow 3Zr + 4RECl_3(LiCl - KCl)$$
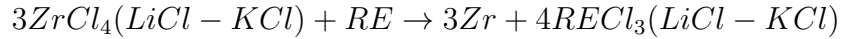
This process is shown to have a decontamination factor of 10 in regards to separating REs from actinides [14]. Additionally, by using Zr as the metal substitute, it is compatible with fuel fabrication later [12].

Electrorefining

Electrorefining is the primary process in pyroprocessing, and is the feed point for fast reactor fuel, since it does not require reduction or chopping. Being the most important process, it is also the most complex with a multitude of input parameters and outputs. The goal of the refining process is to separate the uranium and TRU from the alloy ingot formed in the reduction phase. Two streams will be formed for the fabrication of fuel: one stream that is

a mix of U/TRU at the desired ratio, and the other a pure stream of uranium. The refining step's efficiency relies on temperature and current primarily, however, advanced methods are being developed. KAERI for example has conducted work on adding a central stirrer, lowering pressure, and rotating the anode [4]. The rotation aims to mix the uranium in the salt such that none gets stuck on the bottom or edges of the vessel. Stirring too vigorously, however, can lead to the removal of uranium dendrites from the cathode thereby decreasing efficiency.

The governing reactions that allow this process to work are based on the stability constants and oxidation potential of the remaining FPs. The voltage used, 0.5-1V, is such that Uranium is unstable in the chloride form [10], while TRUs have a higher stability. This leads to TRU remaining in chloride form, along with some uranium, and pure uranium accumulating on the cathode. The chloride reaction follows the below equation, and will run to the right as long as there is uranium within the salt [10].

$$UCl_3 + TRU(RE) \rightarrow U + TRU(RE)Cl_3$$

$$UCl_3 + 3Na \rightarrow 3NaCl + U$$

$$UCl_3 + 3Cs \rightarrow 3CsCl + U$$

$$UCl_3 + Pu \rightarrow PuCl_3 + U \qquad \delta G = -22.44 kcal$$

$$4UCl_3 + 3Zr \rightarrow 3ZrCl_4 + 5U \qquad \delta G = 31.123 kcal$$
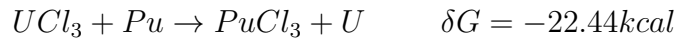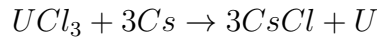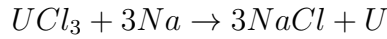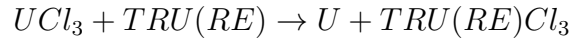
As shown by the reactions above, the TRU have a favorable Gibbs free energy value for spontaneous reactions while the transition metals do not [15]. This leads to the transition metals remaining in the anode basket while the TRU are drawn into the liquid cadmium cathode [16].

Electrowinning

The electrorefiner accumulates TRUs and rare earth fission products within the salt. These isotopes build up and require separation and disposal, therefore the salt from the refiner is sent to the electrowinner. This stage further purifies the salt by targeting the electric potential of TRUs, RE, and U again [16, 10]. Placed in liquid cadmium once again, the three groups have overlapping electric potentials leading them all to deposit in the cadmium [16]. While the refiner's role is to generate a stream of pure uranium, the electrowinner performs co-extraction of Uranium and TRUs. This inherent proliferation resistance is a main draw of the pyroprocessing technique. Rare earths are still present on the cadmium and further separations must be conducted. These elements are removed through the addition of $CdCl_2$ which oxidizes the rare earths, while the uranium and TRUs are unaffected. These oxidized elements fall back into the salt, leaving the purified U/TRU stream on the electrowinner.

Although the facility is great in terms of safeguards, pyroprocessing has its share of drawbacks as well. Currently, pyroprocessing can only be performed as a batch process, which significantly limits throughput compared to a continuous facility. Additionally, the safety and economic concerns of running a molten salt plant are much greater than a nitric acid one. Despite these downsides, pyroprocessing is an efficient use of electrochemical separation and a leader in proliferation resistant separations.

There are multiple different designs for a pyroprocessing facility, the most prominent being from ANL, INL, and KAERI. In order to encompass them all, we must take a generic approach. This is accomplished by including the following sub-processes: voloxidation, electroreduction, electrorefining, and electrowinning. While electrorefining is the process of primary concern, each of the processes has an important in role in various processing plants.

1.3 Goals

The goals of this work are to appropriately model a generic pyroprocessing facility with medium fidelity capable of diversion. With this model in CYCLUS we wish to explore the capability of modeling sub-facilities and diversion. In addition, we will use this higher fidelity model to verify transition scenarios such as EG01-EG24 within CYCLUS [8]. Finally we wish to evaluate optimum detector placement and measurement points for various facility layouts through sensitivity analysis.

Chapter 2

Methods

2.1 Cyclus

CYCLUS is a modular, agent-based nuclear fuel cycle simulator that models the flow of material through user-defined nuclear fuel cycle scenarios. CYCAMORE, the CYClus Additional MOdules REpository, provides common facility archetypes (separations, enrichment, reactor, etc.) [17]. The CYCLUS framework provides benefits compared to other fuel cycle simulators, some being the open source nature, modular capabilities, and use of agents. Customizable agents populate simulations, allowing for a diverse use case. Exact isotopes are dynamically tracked between facilities in discrete time steps [2]. Isotope tracking is a key aspect of CYCLUS that we will use for signatures and observables, in addition to allowing burn-up calculations in more complex fuel cycle scenarios.

2.1.1 Open Source

Many fuel cycle simulators are restricted to industry licenses or the national labs that developed them such as ORION, VISION, or COSI. This restricts nuclear fuel cycle simulator use and development in academia, therefore a tool such as CYCLUS fills a necessary gap. The CYCLUS framework relies on free libraries and open development that allows continuous contributions from various universities and fields of research. This increased accessibility allows more diverse use and expansion on the simulator as seen with codes like CyBORG and Bright-Lite.
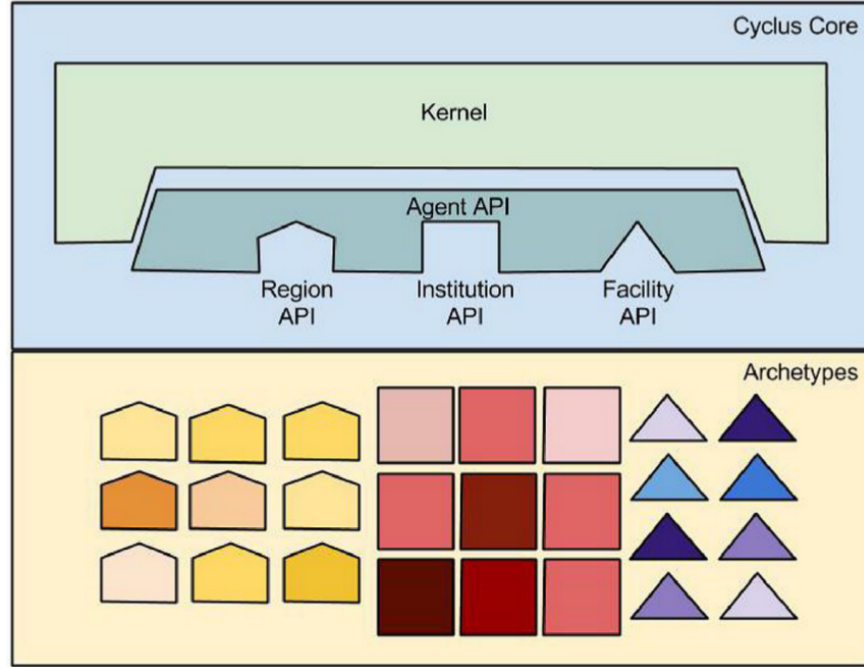
Figure 2.1: Visualization of Cyclus API for modular facilities, regions, and institutions [2].

2.1.2 Modular

The modularity of Cyclus also contributes to the customizability of fuel cycle scenarios. Rather than having locked material connections between facilities, the modular Cyclus scenarios allow easy implementation of new connections. This is handled through the use of a dynamic resource exchange (DRE) in the Cyclus kernel. The DRE uses a system of material offers and requests to find the best connections at each time step. Figure 2.1 demonstrates how the agent API is used to mediate the Cyclus kernel's DRE and the implementation of each agent.

The structure seen in Figure 2.1 is largely responsible for the breadth of agent types of varying fidelity. Provided new agents have the appropriate material trade offers and requests, facilities can be designed to any required fidelity.

2.1.3 Archetypes

Agents contain a hierarchy of *regions, institutions, and facilities* such that *regions* hold one or more *institutions*. Similarly, *institutions* control *facilities* necessary for the actual fuel cycle. For this work, we are most interested in the implementation of *facilities* - particularly how they are defined. Nuclear fuel cycles contain multiple variations of the same facility requiring a diverse collection of pre-designed facility process models, known as *archetypes*. These archetypes are used to define the physics and behavior of specific facility types such as reactors, reprocessing, enrichment, etc. Archetypes with pre-defined parameters are referred to as prototypes (an AP1000 for example is a prototype). Furthermore, facilities are prototypes that have been given specific data such as deployment time, location, lifetime, etc.

2.2 Signatures and Observables

Before constructing a pyroprocessing archetype, appropriate signatures and observables must be determined to set as our input parameters. To identify signatures and observables found in a variety of pyroprocessing plants, we expand upon what was discussed in chapter 1 by looking at experimental data from electrochemical plants. The primary resources are from INL, KAERI, and ANL [16, 18, 3, 19]. We break up these parameters into two distinct categories: direct and indirect, corresponding to signatures and observables, respectively. If the inspector has direct access to material these are referred to as signatures, whereas, indirect monitoring, such as power draw or thermal imaging, represent a lower level of access.

2.2.1 Material Balance

Voloxidation

Light Water Reactor (LWR) fuel must be treated and separated before proceeding with electrolytic processes. Uranium dioxide heated to 500°C is converted to U_3O_8 while noble

gases, carbon, and tritium are collected to decay in storage. Actinides are also converted to their stable oxide forms and a majority are removed [18, 11]. Heating uranium dioxide above 800°C increases voloxidation throughput. Cycling oxidants between H_2 and air also improves the U_3O_8 reaction rate [11].
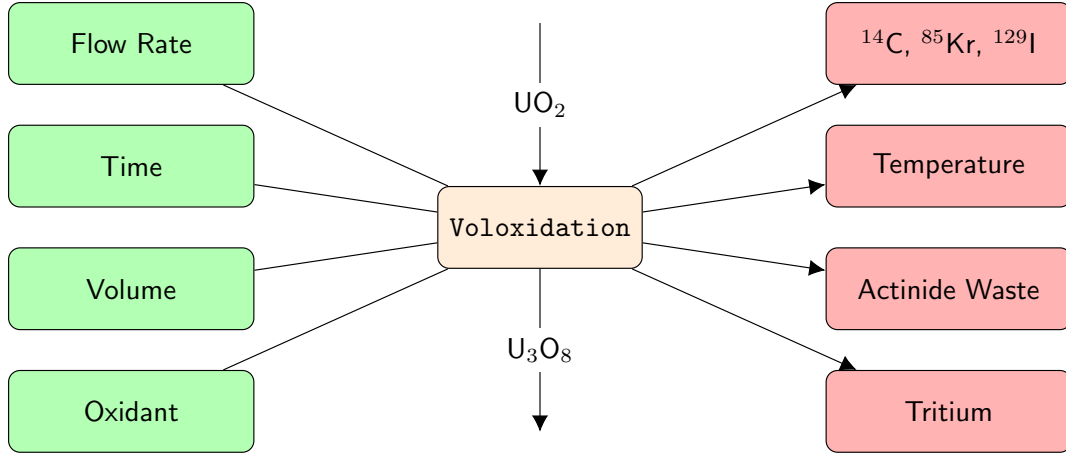

Figure 2.2: Voloxidation material balance area [11].

Electroreduction

The oxidant is converted into metallic fuel through electroreduction to be further refined through electrorefining and electrowinning. Yellowcake, created in voloxidation, enters the cathode, a negatively charged metal basket. A current density between 100 and 500 mA/cm² is applied to the anode in a molten LiCl salt. The electrolytic reduction process primarily results in diffusion of Cs, Ba and Sr, along with reduction and conversion of Zr into metallic form [20, 18]. Electroreduction can further improve its throughput by adding Li_2O as a catalyst; this catalyst also prevents dissolution of the anode [20]. Since Li_2O is used to speed up the reaction, the operators could add more oxide than reported to International Atomic Energy Agency (IAEA). More frequent shipments of lithium oxide can be tracked as an observable to match records.
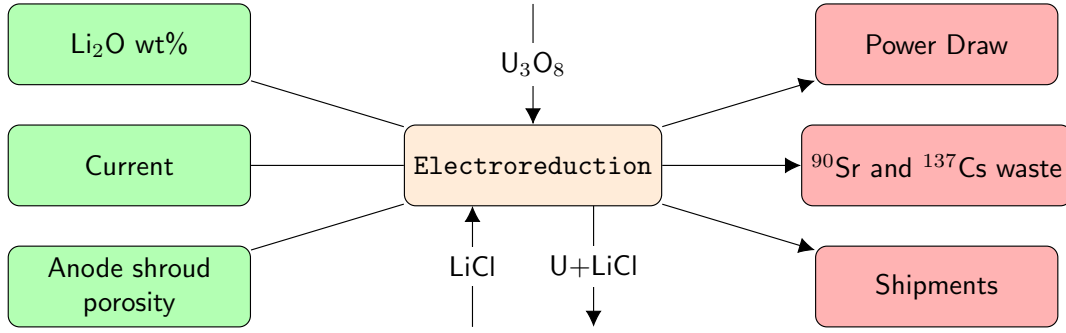
Figure 2.3: Reduction material balance area [21].

Electrorefiner

Once in metallic form, electrorefining electrochemically separates uranium and TRUs for fuel fabrication. The uranium and salt mixture from reduction is fed into an anode basket suspended in a graphite cathode. A LiCl-KCl eutectic is used as an electrolyte above 500°C [18, 16]. Uranium dissolves at the anode to recombine at the cathode as metallic uranium. Waste TRUs and lanthanides are in a soluble chloride form while fission products and cladding remain in the anode basket. Finally, actinides and fission products are removed from the cladding electrochemically [16].

Lee et al. [21] show decreasing system pressure improves removal efficiency. Temperature, however, exhibits the opposite effect: as temperature decreases so does salt removal. This comes into effect particularly depending on instrumentation and containment material choice [21]. Iron, for example, limits operating temperature because a eutectic forms at 725°C [22]. In facilities where iron equipment is present, temperatures are limited to 700°C, hindering efficiency. Cathode arrangement and anode rotation speed also affect the collection of uranium dendrites [21]. A central stirrer mixes uranium dendrites stuck on the vessel, improving separation efficiency and increasing throughput.

The electrorefining process also produces a fission product waste stream which requires monitoring. The following products are produced and tracked in Pyro Reprocessing Module (PyRe) at this step: Tc, Ag, Pd, Rh, Ru, Mo, and Zr [18]. Uranium and transuranic (TRU)
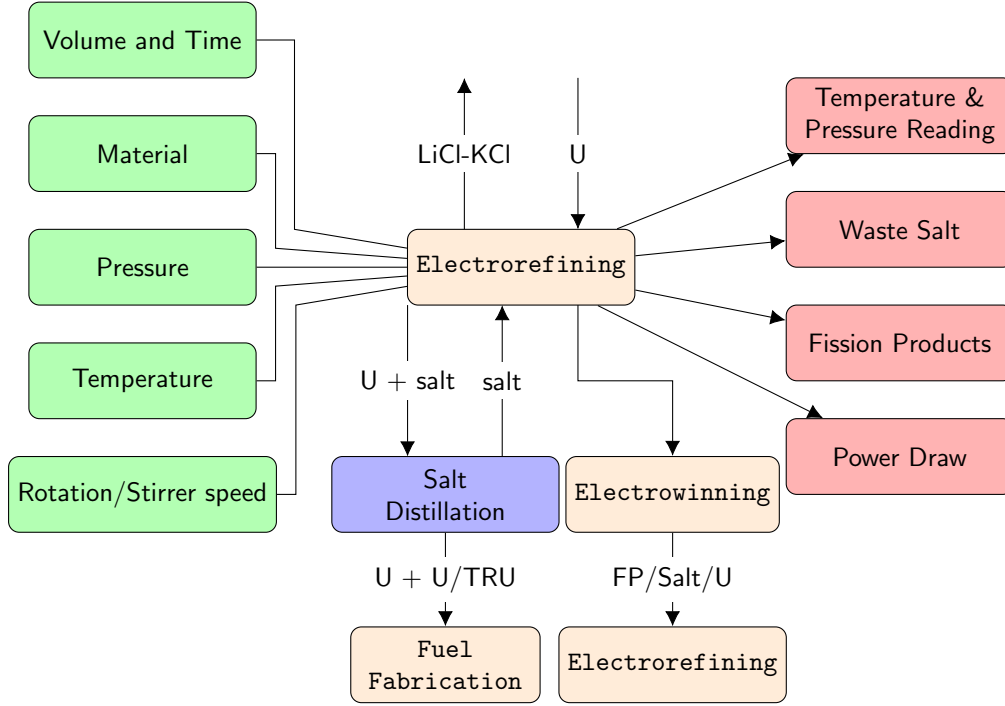
Figure 2.4: Refining material balance area [21].

product streams separated at this stage are sent to fuel fabrication, while the remaining salt is reformed as an oxidant and recirculated. Separation efficiencies are taken after recirculation and treated as a once-through cycle.

Electrowinner

Molten salt containing TRUs from electrorefining is separated through electrowinning. This process separates trace uranium quantities, lanthanides and fission products. At 500°C there is approximately 99 wt% reduction in actinides and lanthanides [18]. Throughput also depends on material choice for the inert electrodes, impacting separation efficiency [23]. A shroud surrounds the anode to provide a path for O^{2-} ions to the anode and prevent Cl_2 from corroding the anode [24, 20]. Optimum operating current depends on material choice for the anode shroud since a nonporous shroud limits ion pathways to the anode contact points. Higher porosity corresponds to free ion paths and a higher current. Increased currents reduce

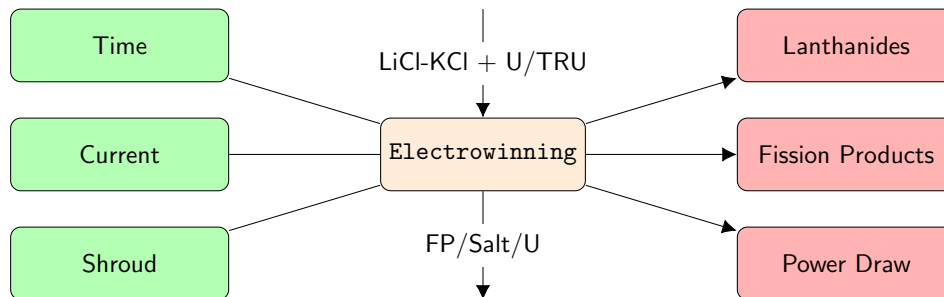the separation time for electroreduction and electrowinning [20].

Figure 2.5: Winning material balance area.

2.2.2 Signatures

Potentially trackable signatures and observables include truck deliveries and power draw [25, 26]. This list is expanded upon in Table 2.1 to include pyroprocessing parameters. For this work we narrow down the list to more facility specific parameters rather than observables like the parking lot or truck movement. We also use this table to determine the most common operational settings such as temperature, pressure, current and flow rate.

2.2.3 Waste Forms

Waste from pyroprocessing is split into 3 main waste streams in which we can directly measure their *signatures*. Signatures require direct access to the waste streams to monitor. These techniques vary depending on the waste form. Leading approaches include non-destructive assay, multiplicity counting, and a plutonium to curium ratio measurement [28, 29].

Sub-process	Parameters	S & O	Refs
Voloxidation	Volume	Tritium	[11]
	Oxidant	^{14}C	[18]
	Flow Rate	^{129}I	
	Temperature	^{85}Kr	
	Time	Actinides	
Electroreduction	Volume	^{90}Sr	[7]
	Batch Size	^{135}Cs	[18]
	Li$_2$O wt%	^{137}Cs	[20]
	Current	Power Draw	[16]
	Porosity	Shipments	[27]
	Distillation Speed	Throughput	
	Time		
Electrorefining	Volume	Fission Products	[21]
	Time	Power Draw	[16]
	Material	Waste Salt	[18]
	Anode Rotation	Vacuum Pressure	[23]
	Stirrer Speed	Temperature	[24]
	Pressure	Throughput	
	Temperature		
Electrowinning	Current	Power Draw	[18]
	Shroud Material	Cadmium Waste	[16]
	Time	Fission Products	[7]
	Flow Rate	Lanthanides	
		^{135}Cs	
		^{137}Cs	
Facility	Throughput	Shipments	
	Batch Size	Parking Lot	
		Thermal Image	

Table 2.1: Archetype inputs and signatures & observables at each sub-process.

2.3 Pyre

As per the goal of this project, Pyre was designed such that multiple potential pyroprocessing facilities can be modeled at medium fidelity. To accomplish this, and improve upon the lower fidelity of the separations archetype found in CYCAMORE, we inform our separation efficiencies with higher fidelity models including SSPM and AMPYRE [30, 31]. The below Figure 2.6 incorporates material balances for each sub-process and highlights some key parameters we either use in the input file or look at for diversion.

2.3.1   Structure of Pyre

The archetype separates each sub-process to be handled independently, letting the user determine which aspects are necessary for their facility. We took this approach to also allow for better handling of various waste streams. Ceramic waste must go through the electroreductor, whereas metallic fuel can go straight into the electrorefiner [3].

Governing Pyre Class

The archetype separates each sub-process to be handled independently, letting the user determine which aspects are necessary for their facility. Each sub-process is capable of handling its own diversion and material tracking. The streams produced from these processes are sent further through the facility, and the wastes are recorded. Waste streams are used to verify nominal operation before being traded to a storage facility. Product streams are further refined by each sub-process until the fuel fabrication stage. The pure uranium stream and U/TRU stream are then offered up for trade with a fuel fabricator.

Diverter

Figure 2.7 shows the difference between nefarious diversion, in gray, and operator diversion, in orange. The gray line shows normal operation where diversion occurs through the shipment, and can be detected by a discrepancy in shipment records. The more difficult case to handle, shown in orange, imagines an inside man altering operational settings to increase product over reported quantities. The scenario we are concerned with is operator diversion; we wish to determine the most important points in the plant to monitor for potential diversion. A side effect of this goal is that we must be able to detect diversion by changing key operational settings.

CYCLUS does not natively handle diversion from inside facilities as required for the goals for Pyre. We implemented a higher fidelity diversion model through the diverter class to handle operator and nefarious diversion. This class is specific to the Pyre archetype currently,

as the diversion facility must be set up to allow it. The diverter class' goal is to inform the Pyre facility what parameters are being changed to divert material. The algorithm used for this can be seen in Figure 2.8 which inputs the sub-process that contains an inside man, the parameters he has access to, and how much material he wishes to divert. The diverter directs this information to the appropriate sub-process which then uses a bisection function to determine the parameter value associated with the new product.

2.3.2 User Input

Pyre, as with all CYCLUS archetypes, is fully configurable through the text based input file. The input consists of the operational settings shown in Table 2.1 and the separation efficiency for each isotope. The efficiencies input for each sub-process corresponds to that facility's ideal state. Operational settings act as a capacity factor, reducing the overall efficiency to match those seen in test facilities. This input structure allows users to follow predefined example facilities, or input their own separation efficiencies.

2.4 Testing

2.4.1 Reproducibility

Cooperation and co-development are a major part of open source development. As such, any addition to open source code in particular should be well tested for outside developers. Thorough testing allows concurrent or future developers to maintain and expand the project while ensuring all capabilities are maintained. Following these guidelines, a number of tests verifying trade capability and sub-process physics are added to ensure reproducibility. The details of these verifications will be explained further in Chapter 3.
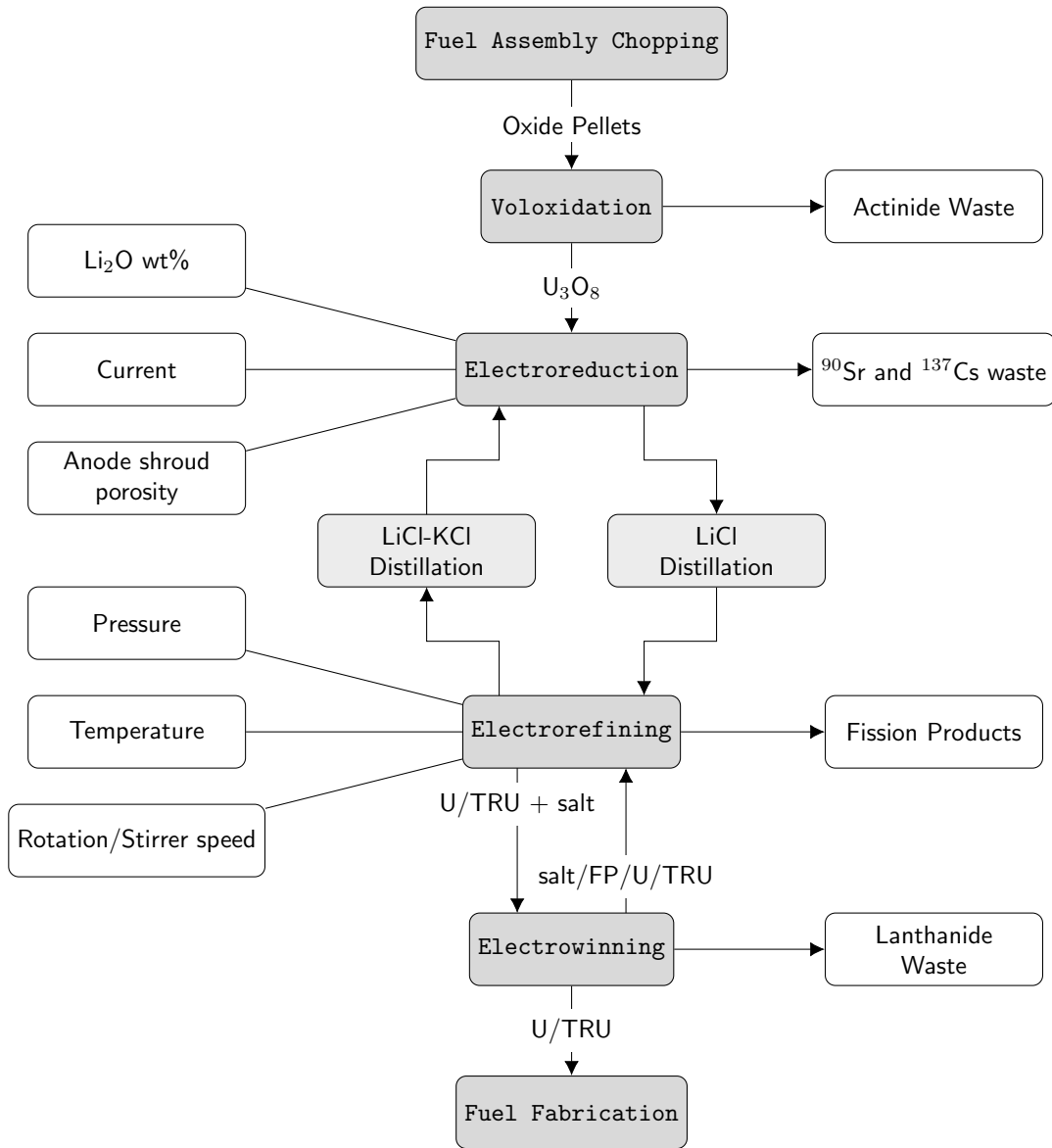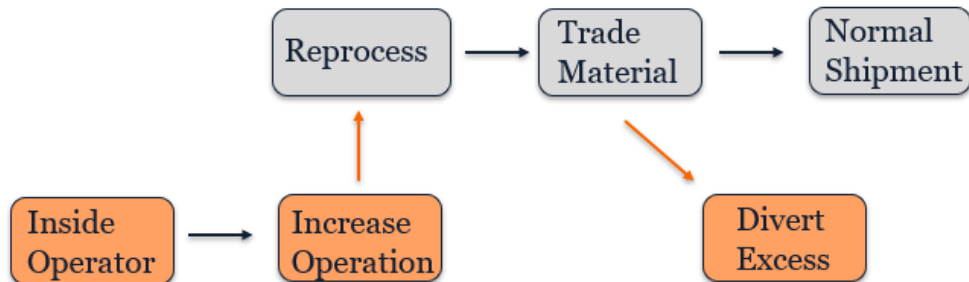
Figure 2.6: Pyre material flowchart [7].

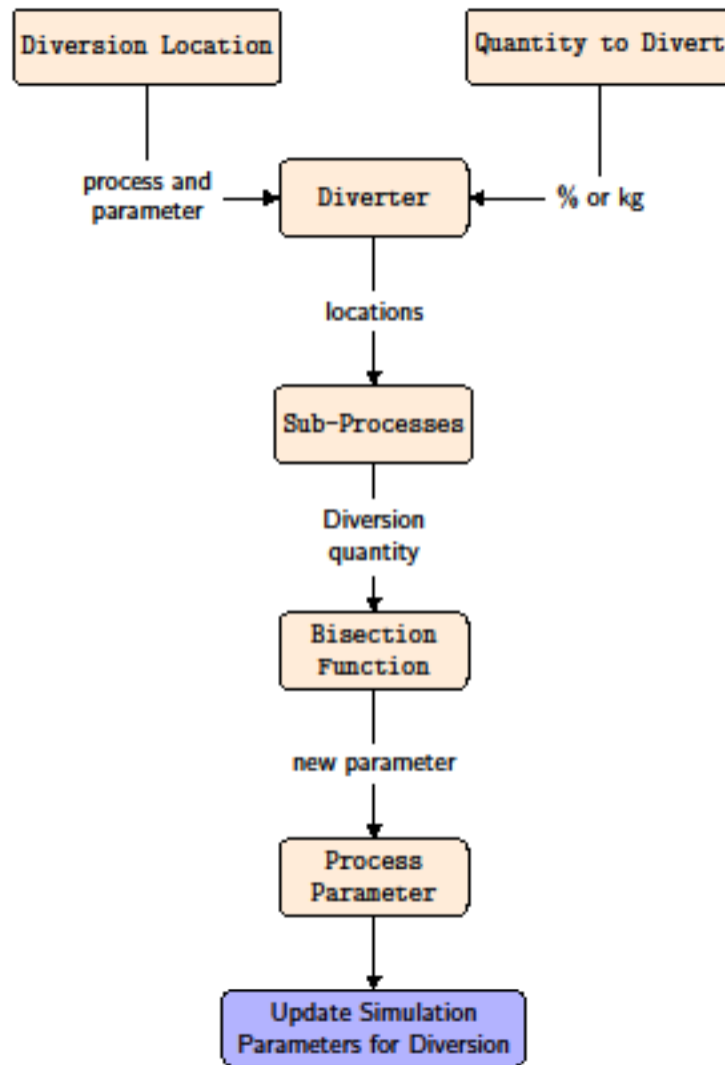Figure 2.7: A flowchart demonstrating the main forms of material diversion.

Figure 2.8: Pyre diverter class flowchart.

Chapter 3

Simulating Fuel Cycles

3.1 Simple Verification

Several simulations were run to verify the capabilities described of Pyre. Before considering complex fuel cycles, we must first verify capabilities within Cyclus. Cyclus archetypes are expected to meet a number of capabilities such as trading, decommissioning, and isotope tracking. To demonstrate these functionalities we ran a simple scenario with one source, sink, and pyre facility. The pyre facility is run at default values corresponding to an average installation. The source facility provides light water reactor (LWR) waste to separate with a composition given by Duderstadt.
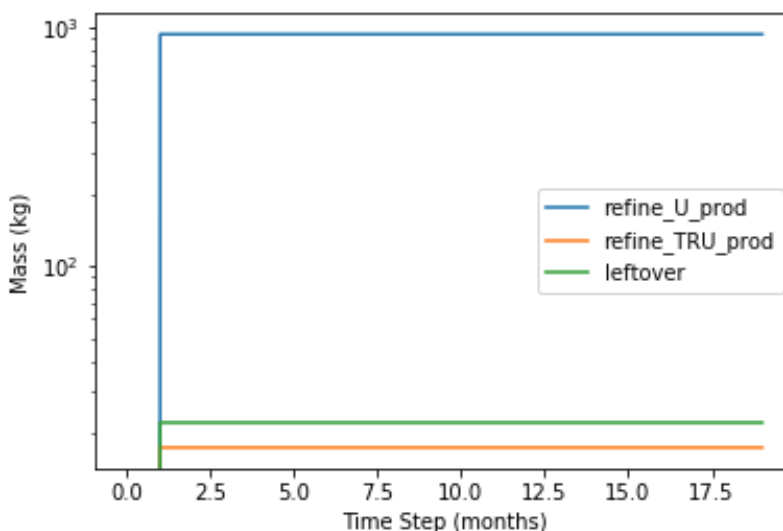

Figure 3.1: Product time series of a simple simulation.

The above Figures 3.1 and 3.2 track the shipment of material from the pyre facility to the
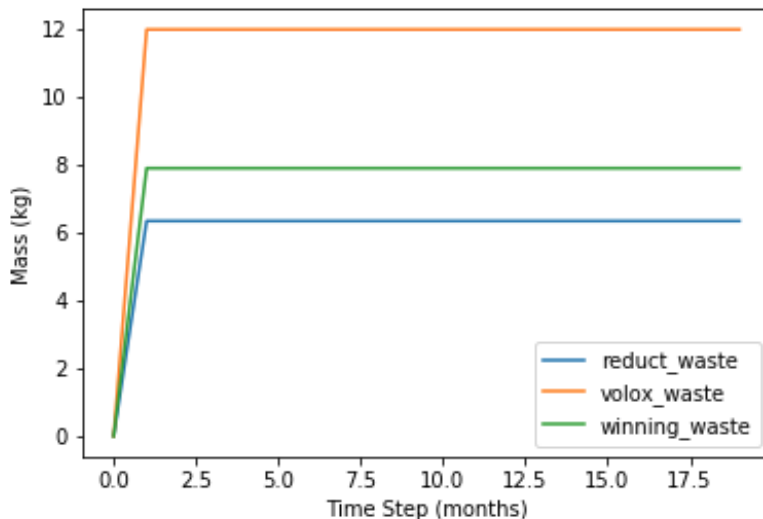
Figure 3.2: Waste time series of a simple simulation.

sink. Individual waste streams are identified and verify the functionality of each sub-process in this LWR configuration. Since the scenario is run with constant parameters and number of facilities, the transactions are expected to remain constant and the above figures meet this expectation. In addition to demonstrating sub-process capabilities, material transactions with other Cyclus facilities can also be observed as expected.

3.1.1 Isotopic Streams

Another key aspect of material transactions is the composition of each shipment. To meet Cyclus standards we must be able to track each isotope for separation and trading with various facilities. This is done in a couple ways within Pyre, the first being various stream types such as waste or product, and the second being isotopic composition within these streams. In Figure 3.3 the 3 waste streams shown in Figure 3.2 are compared isotopically. We do this comparison to further investigate the performance of each sub-process by identifying the appropriate separation of elements. The electrowinner, shown in green, correctly contains heavier elements such as lanthanides while the electroreductor, in red, is responsible for the lighter metals as well as changing oxidation states which is not reflected in these streams.
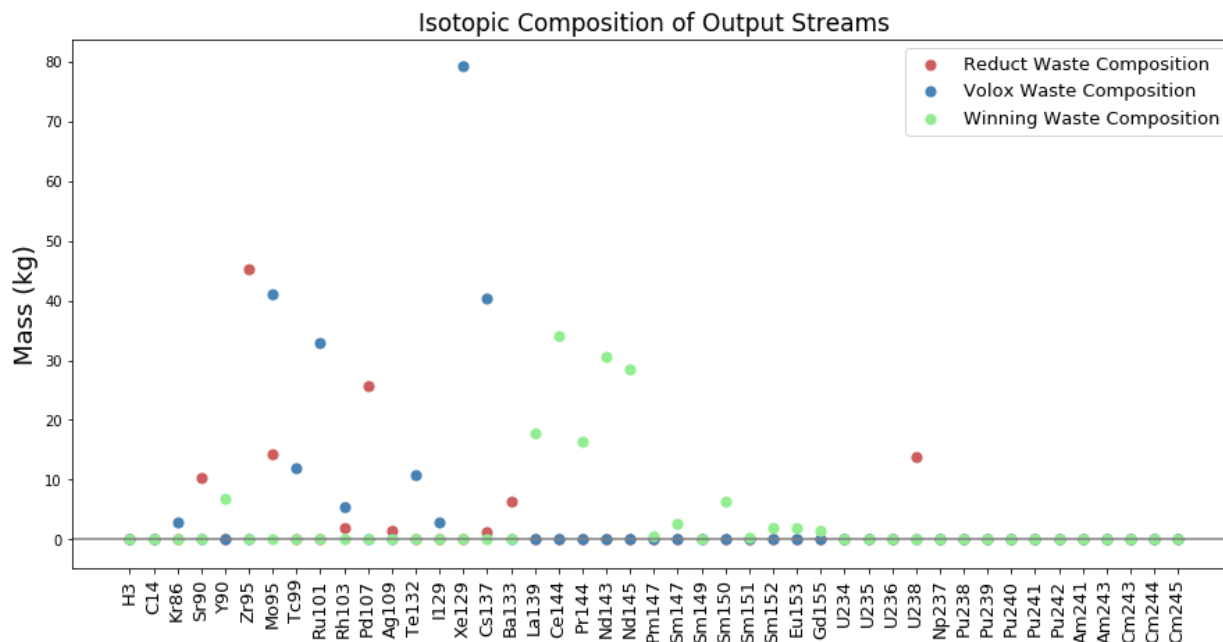
Figure 3.3: Isotopic Composition of Average Waste Streams

3.1.2   Simple Diversion

Figures 3.4 and 3.5 are used to demonstrate simple diversion scenarios. In particular, the scenario run for Figure 3.4 compares the average case with one of increased power draw. Increasing the power draw of the facility affects sub-process currents. Separation efficiency of the reductor and winner is improved by increasing the current in the anode resulting in the material unaccounted for (MUF) shown above. The voloxidation stream is kept on the plot validating only appropriate processes are being affected.

The other diversion scenario explored here is a theoretical maximum diversion scenario in which two scenarios are run: where parameters are set to their maximum and minimum values respectively. Although an unrealistic scenario since diversion is easily detected, the scenario shows us the worst case scenario and could be used to inform inspection intervals. Figure 3.5 shows that after a 20 month scenario, approximately a significant quantity of plutonium is unaccounted for. As such, inspections would need to occur at a similar interval, depending on the reported capacity.
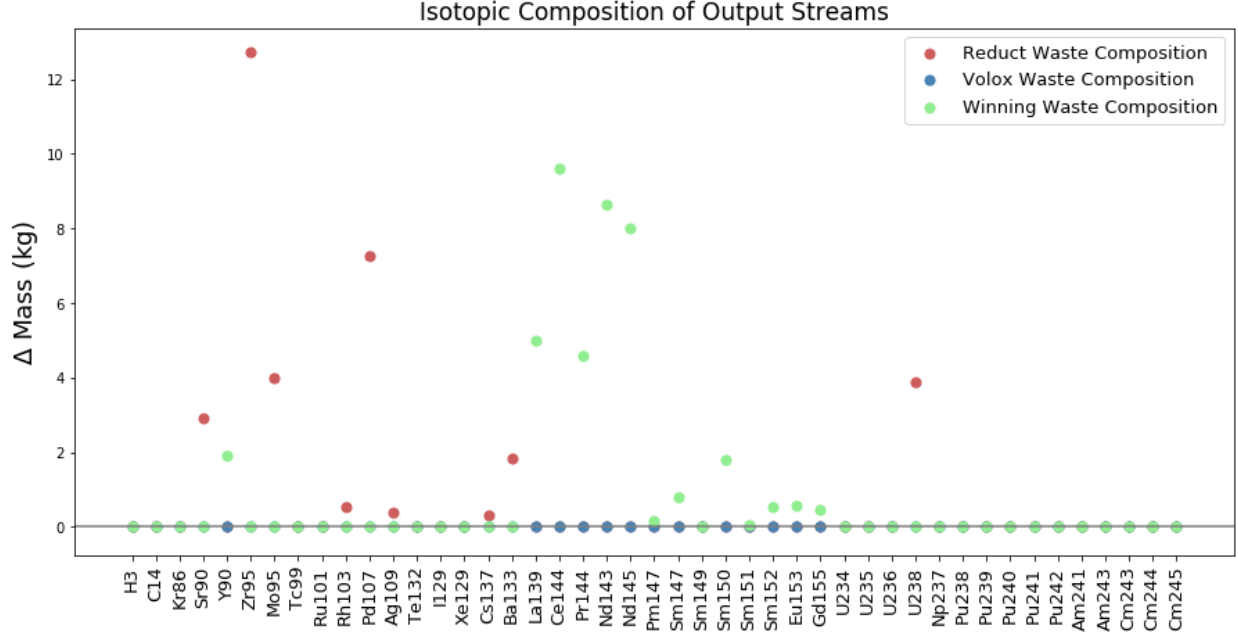
Figure 3.4: Isotopic Composition of Current Diverted Waste Streams

3.2   US Fuel Cycle Transition

After testing the capabilities of Pyre in a small scenario, we implement the archetype in the EG01-EG24 transition scenario described in the goals of this work.

Details	Value	Unit
Simulation start	1959	years
Simulation end	2215	years
LWR Lifetime	60	years
50% of LWRs	80	years
Transition start	2015	years
Reprocessing Facility	PRIDE Pyre	–
New LWR lifetime	80	years
SFR Lifetime	80	years
SFR breeding ratio	1.014	–
Reprocessing Facility	INL Pyre	–

Table 3.1: Transition Scenario setup and details.

Table 3.1 shows the setup for a sodium fast reactor (SFR) transition. In addition to the above information, the scenario is initiated with 200 LWRs with another 200 being deployed in 2015 at the transition period. Two Pyre prototypes are deployed to handle the different
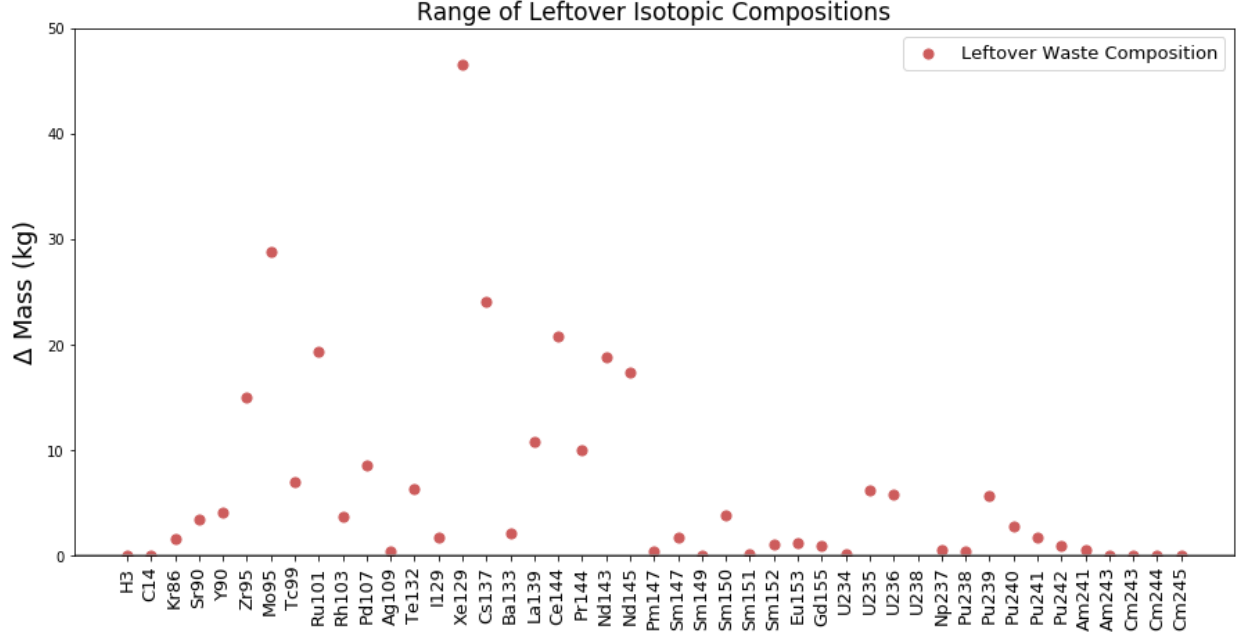
Figure 3.5: Range of Isotopic Values for maximum potential diversion.

fuel types seen in the above scenario. The PRIDE-based facility is configured to reprocess ceramic LWR waste while the INL-based facility handles metallic SFR fuel, and is deployed after the transition.

Figure 3.6 demonstrates the deployment and decommissioning of reactors in this scenario. In order to meet the average 1% annual power growth, additional reactors are necessary while appropriate SFR fuel quantities are accumulated.

3.2.1 Pyre Performance

To verify functionality of the Pyre archetype, rather than the transition scenario itself, we take a look at the fuel production and utilization rather than facility deployment. Figures 3.7 and 3.8 demonstrate the appropriate reprocessing and fabrication of SFR fuel. Figure 3.7 shows the SFR pyroprocessing plants begin producing a sustainable amount of fuel around year 2125. Since all SFRs are breeders in this scenario, we can see that as more reactors are deployed the TRU stock increases exponentially at year 2150. Similarly, the overall utilization of uranium improves as reprocessing is heavily used.
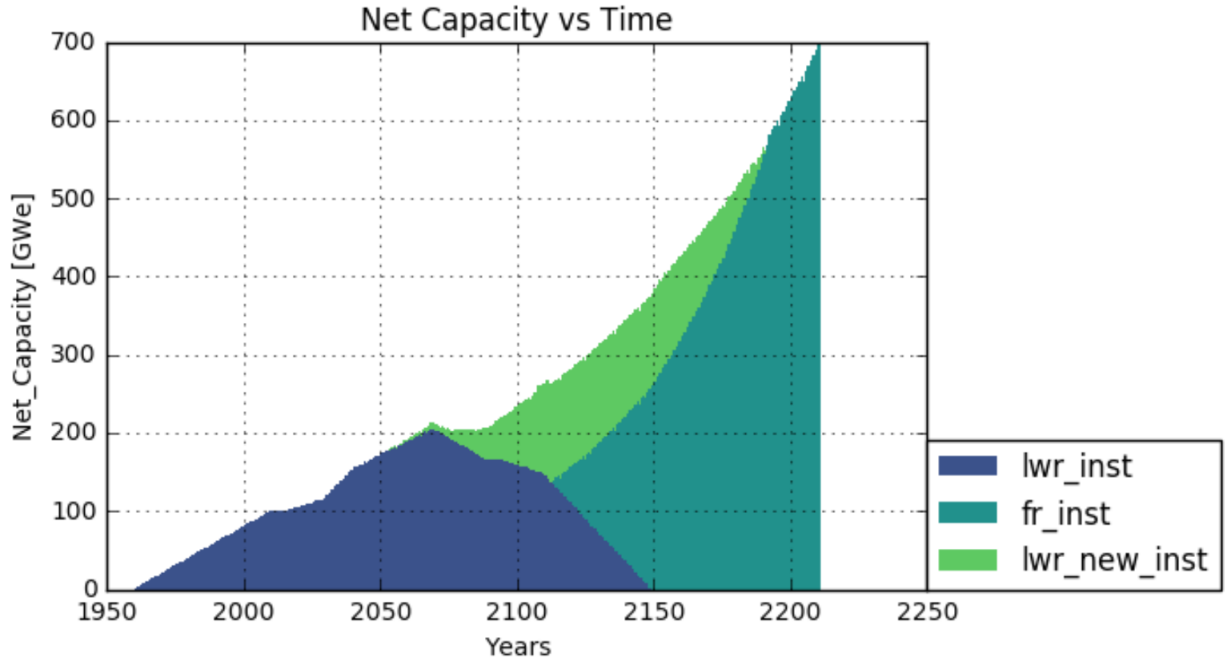
27

Figure 3.6: Net Power Capacity over Time

Figure 3.9 illustrates the complete transition from LWRs and UOX fuel to SFRs at year 2180. As seen in Figures 3.7 and 3.8, TRU fuel production has increased enough to self-sustain the next generation of SFR reactors and decommission remaining LWRs.
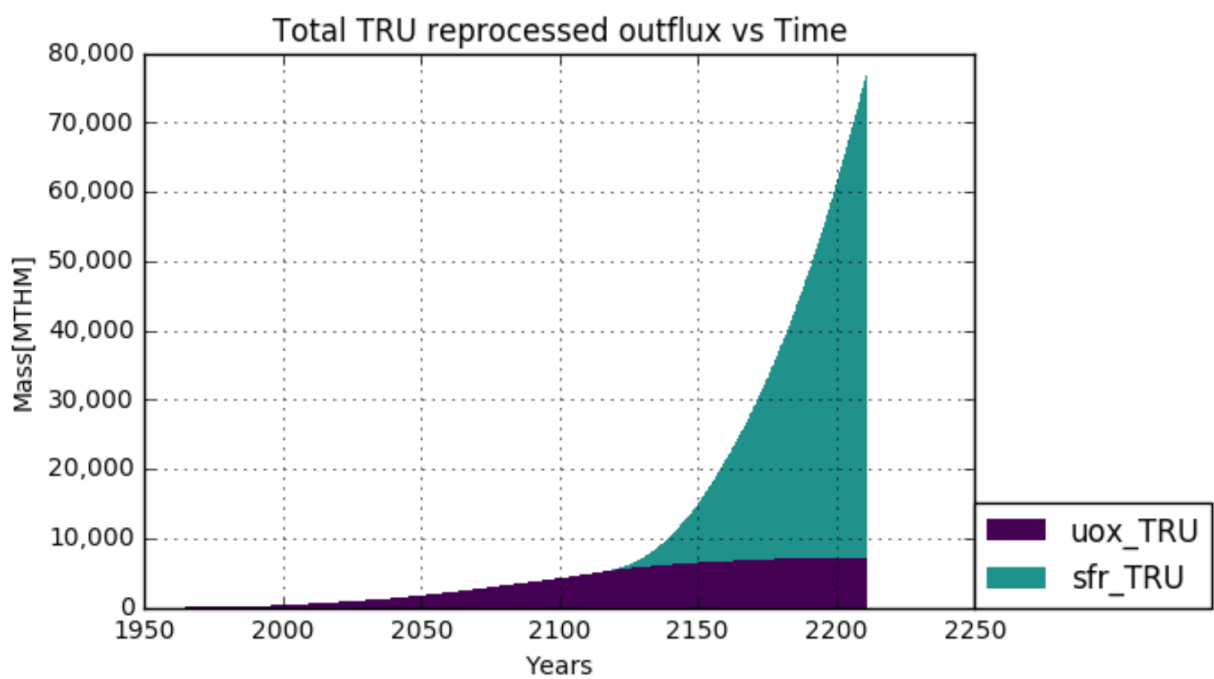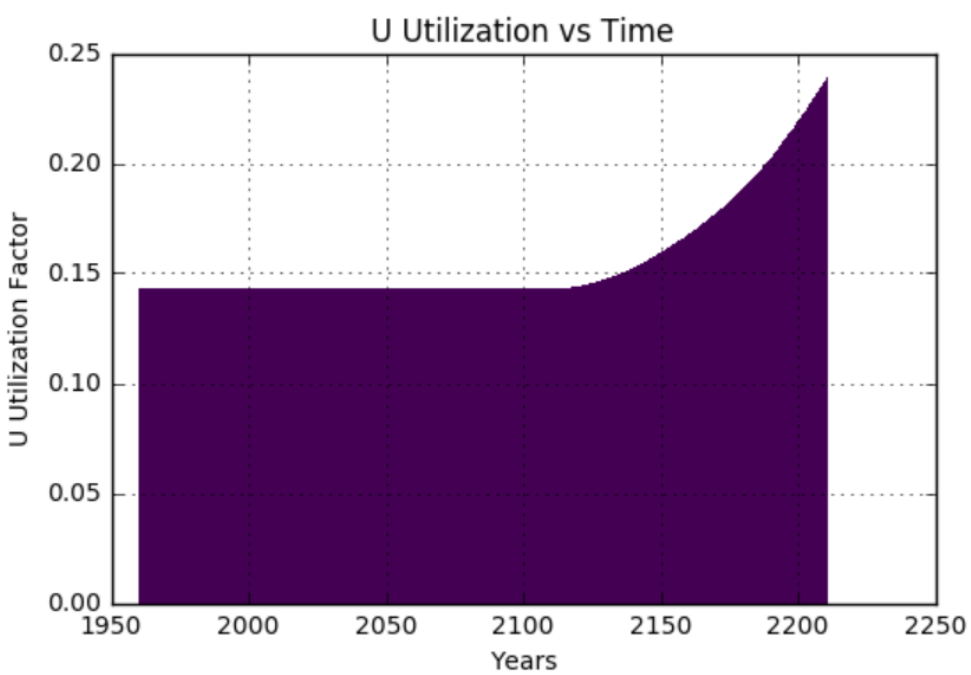
Figure 3.7: TRU utilization over time.
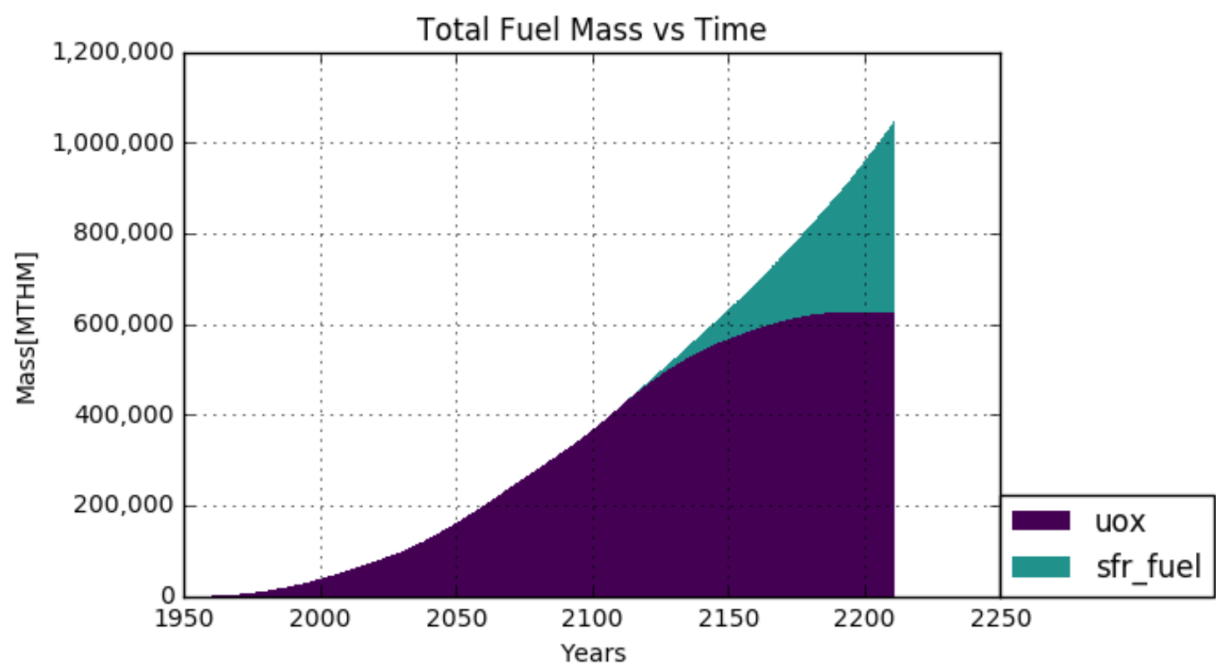

Figure 3.8: Uranium utilization over time.

Figure 3.9: Mass of Fuel Types over Time

Chapter 4

Diversion Detection

The second aspect of this work is identifying potential places for diversion in a generic pyroprocessing facility. We took 2 primary approaches for this work, applying a cumulative sum detection algorithm and performing sensitivity analysis on key facility parameters.

4.1 Cumulative Sum

4.1.1 Requirements of Diversion Detection

The cumulative sum method (CUSUM) applied to Pyre was chosen to fit the following requirements: function with minimal prior information, have online diversion detection capabilities, and fit a modular approach. The CUSUM change detection algorithm relies on developing an expected mean value of a data stream as shown by the following equations [?].

$$f_{t+1} = max(0, f_t + x_t - \mu - \delta)$$

Where:

$$x_t = observed\ data$$

$$\mu = approximated\ mean$$

$$\delta = acceptable\ change$$

This general function adds new observed values to the calculated mean. If the value is

within region of error, typically 3σ, change is not reported. We favor this online diversion detection capability in an effort to achieve timely detection goals set by the IAEA [6]. These intermittent inspections only have access to portions of the complete data stream, thus we aim to mimic reality as closely as possible. In addition, we need this algorithm to work on a variety of facilities with different sub-processes active, ruling out a nodal approach seen by [26].

4.1.2 Limitations of selected method

This approach is not without its drawbacks, since there is no prior data assumed we must generate a reasonable mean before being able to detect diversion. For this work we assume a startup time of approximately 6 months before an appropriate mean can be developed. The next limitation faced with this approach is observing one data stream at a time, while real inspections take a wide range of conditions into account. This concern is addressed by using sensitivity analysis, as seen later in this chapter, to inform on the most crucial sub-processes or settings.

CUSUM relies on a variable mean and noise to obscure possible change points. When a simulator knows the exact value at each time step, without human reporting or measurement error, change detection becomes trivial. To combat this issue, noise is artificially created when the CUSUM class reads data. This way Cyclus retains its constant operating value while the change point has potential to be obscured by measurement error. These detector uncertainties are assumed from common non-destructive and destructive assay practices used by the SEE LANL course [].
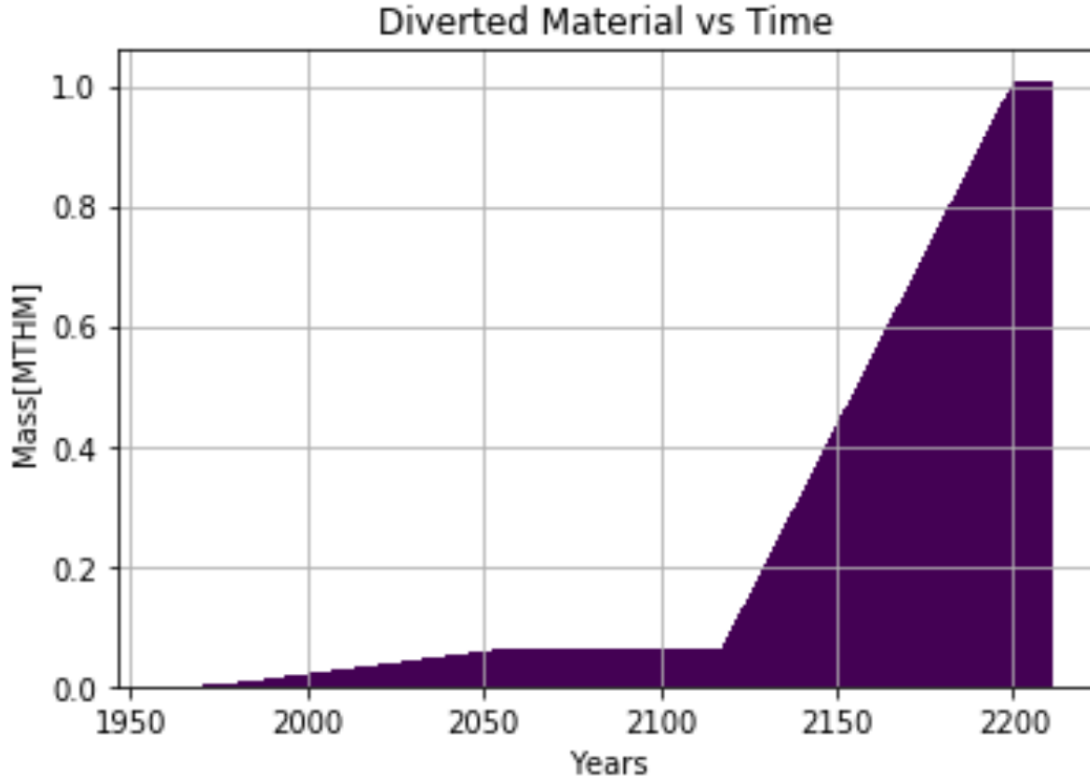
Figure 4.1: A timeseries of diverted material from two Pyre facilities.

4.2 Verification

4.2.1 Nefarious Diversion

4.2.2 Operator Diversion

To test operator diversion capabilities, we ran the EG01-EG24 transition scenario shown in chapter 3 with inside operators. The scenario described in Table 3.1 contains an LWR and SFR configurationg for Pyre. Each prototype siphoned material with different quantities and frequencies to demonstrate its reconfigurability. The LWR Pyre siphoned off 5% every 10 timesteps while the SFR Pyre siphoned off 1% excess every other timestep. Results for this scenario are shown in Figure 4.1.

4.3 Sensitivity Analysis

Sensitivity analysis is an important aspect of this work to know the limits of monitoring these facilities. In this work we use Dakota to alter CYCLUS input files, allowing us to easily run batches of scenarios. To properly use Dakota with CYCLUS, we must use DCWrapper, which uses python to interface between Dakota and CYCLUS' xml input files. Key parameters were run over a range of values for diversion to verify the archetype's capabilities and identify operational ranges. Parameters were selected from the most attractive sub-processes for diversion, the electrorefiner and electrowinner. These two processes are responsible for the production of Uranium and U/TRU ingots, therefore sensitivity analysis was run on each of their key parameters: Temperature, Current, Flowrate, Pressure, Stirrer Speed, and Reprocessing Time.

4.3.1 Temperature

The first setting for consideration is the electrorefiner's temperature. As discussed in methodology, the range for this setting is 500 to 1000 $°C$. However, operation typically occurs above 750 $°C$. For each setting we observe how much material can be diverted within a month; these values can be seen isotopically in Figure 4.2. The stream corresponding to 750 $°C$ is then subtracted from remaining streams to determine the impact of increasing temperature on divertable material. While temperature is a key aspect to the electrorefiner, Figure 4.3 shows that when approaching 1000 $°C$ efficiency does not increase significantly resulting in diminishing returns.

4.3.2 Pressure

Available in advanced electrorefiners, vacuum pressure can improve separation efficiency as well. Similar to our analysis of temperature, isotopic compositions of divertable material can be seen in Figure 4.4. Our baseline for the comparison is atmospheric pressure as this
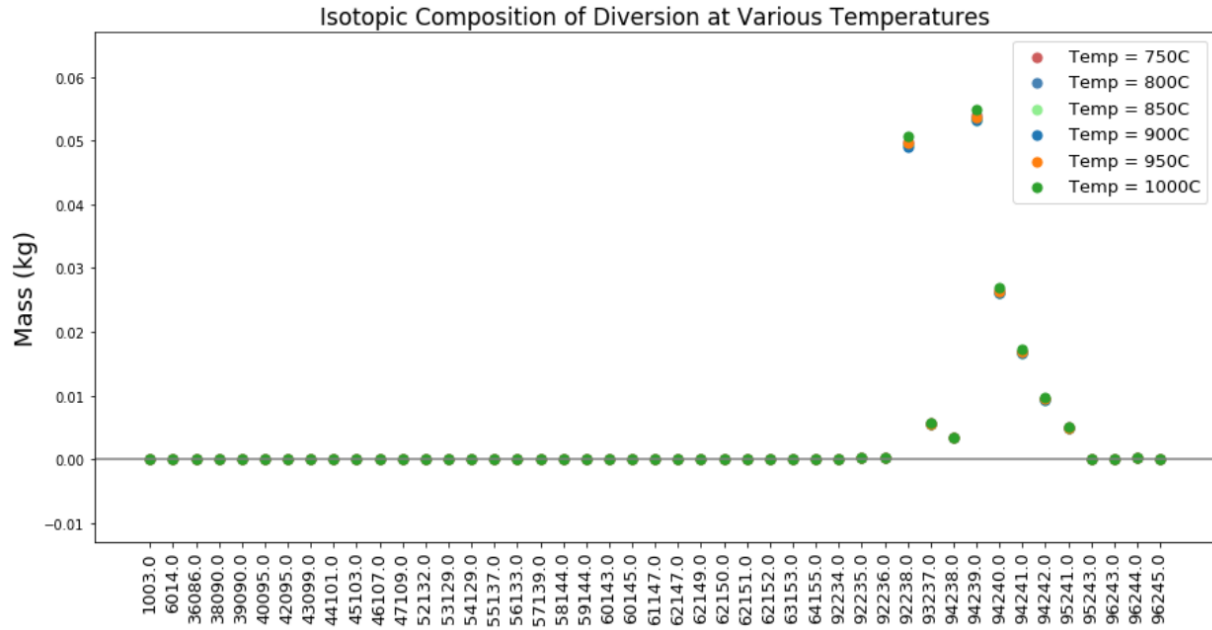
Figure 4.2: Isotopic composition of the Diverted material stream at various Refiner temperatures.
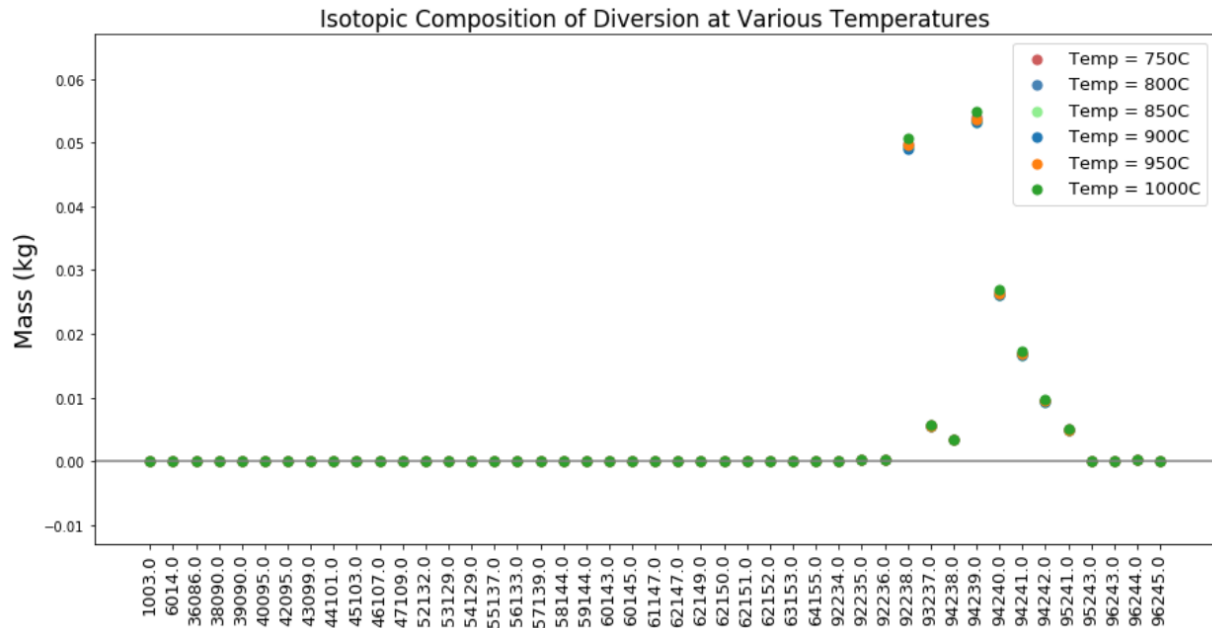

Figure 4.3: Isotopic composition of the Diverted material stream at various Refiner temperatures.
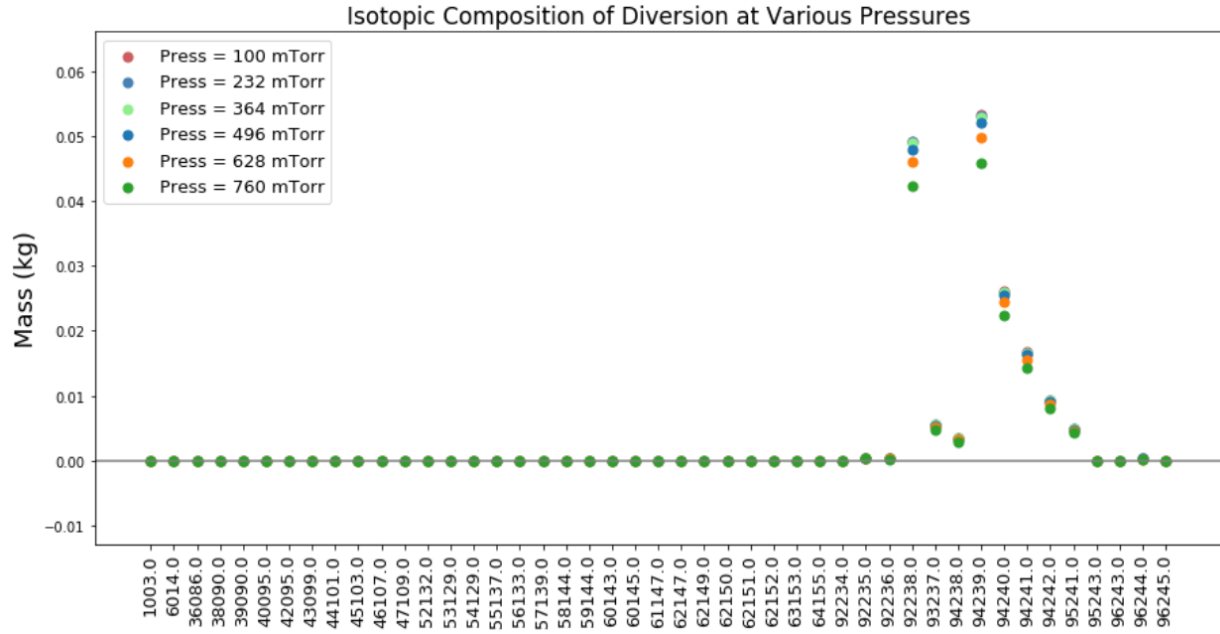
Figure 4.4: Isotopic composition of the Diverted material stream at various Refiner pressures.

will represent facilities lacking this functionality.

4.3.3 Stirrer Speed

4.3.4 Current

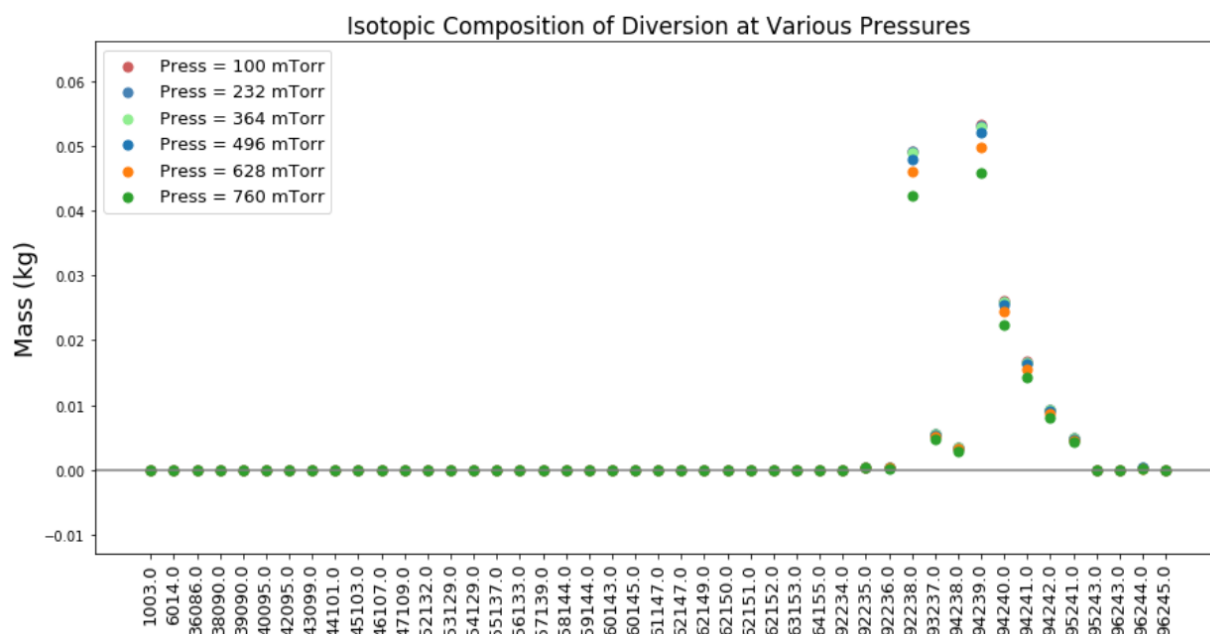### 4.3.5 Flowrate

4.3.6 Reprocessing Time

Figure 4.5: Isotopic composition of the Diverted material stream at various Refiner pressures.
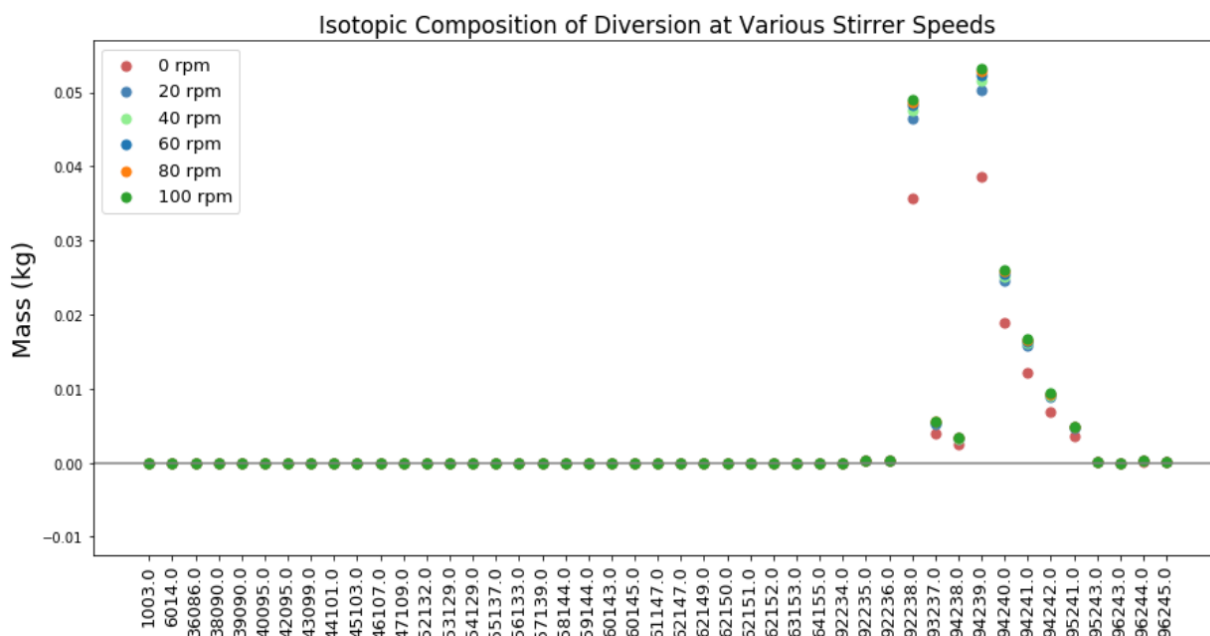

Figure 4.6: Isotopic composition of the Diverted material stream at various central stirrer speeds.
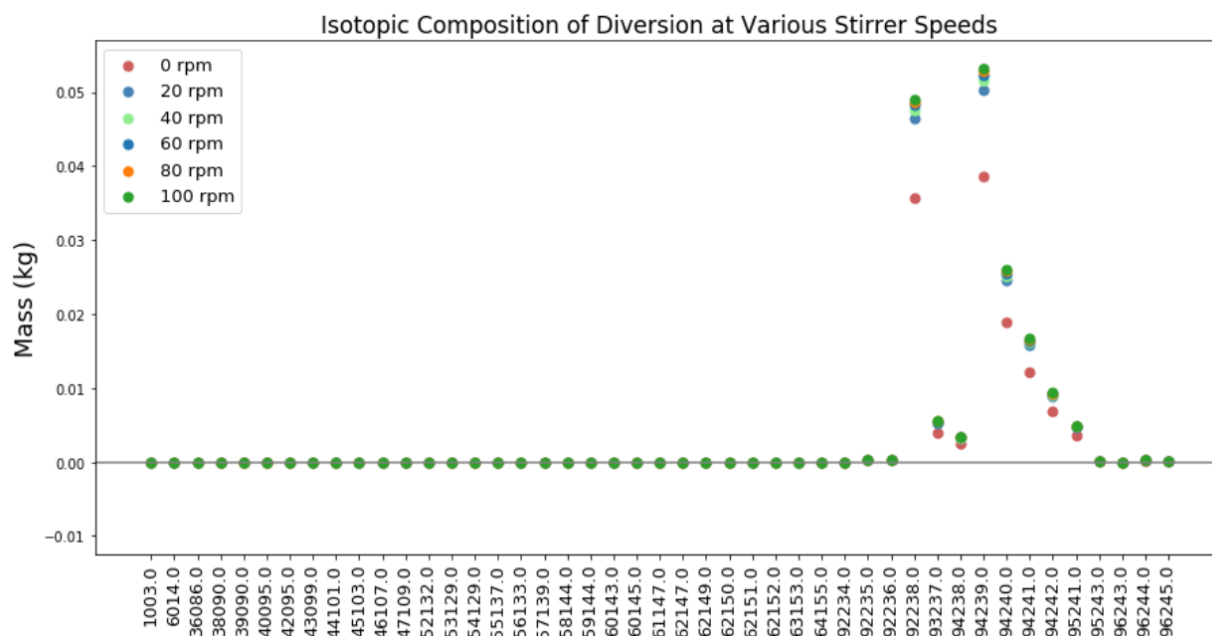
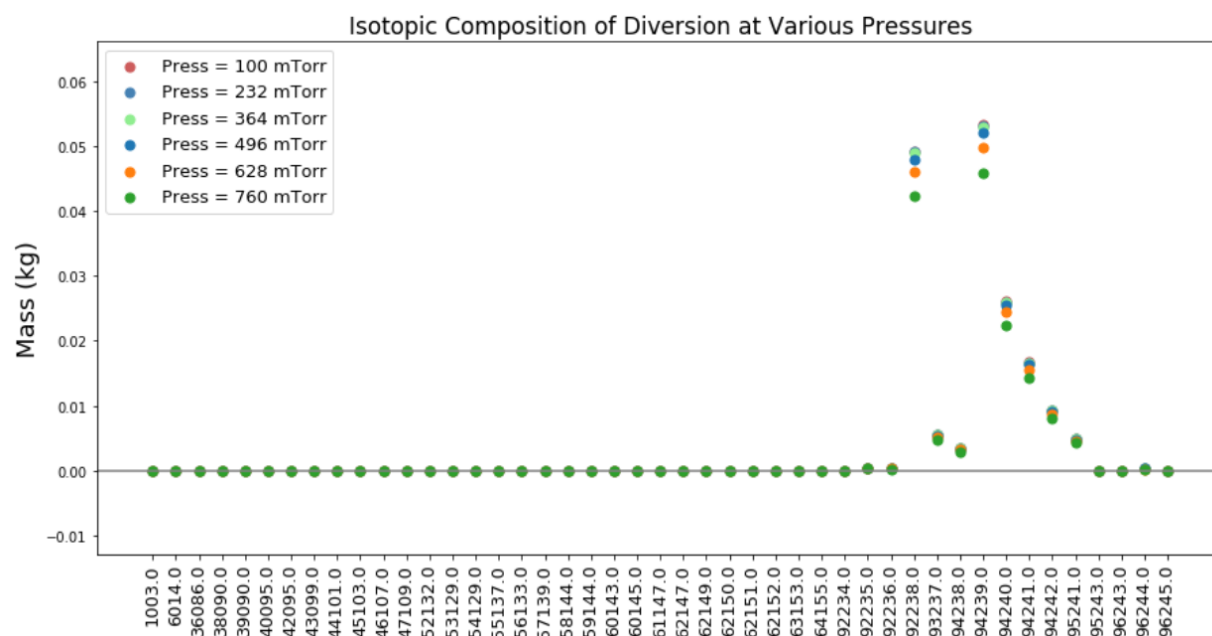Figure 4.7: Isotopic composition of the Diverted material stream at various central stirrer speeds.

Figure 4.8: Isotopic composition of the Diverted material stream at various Electrowinner currents.
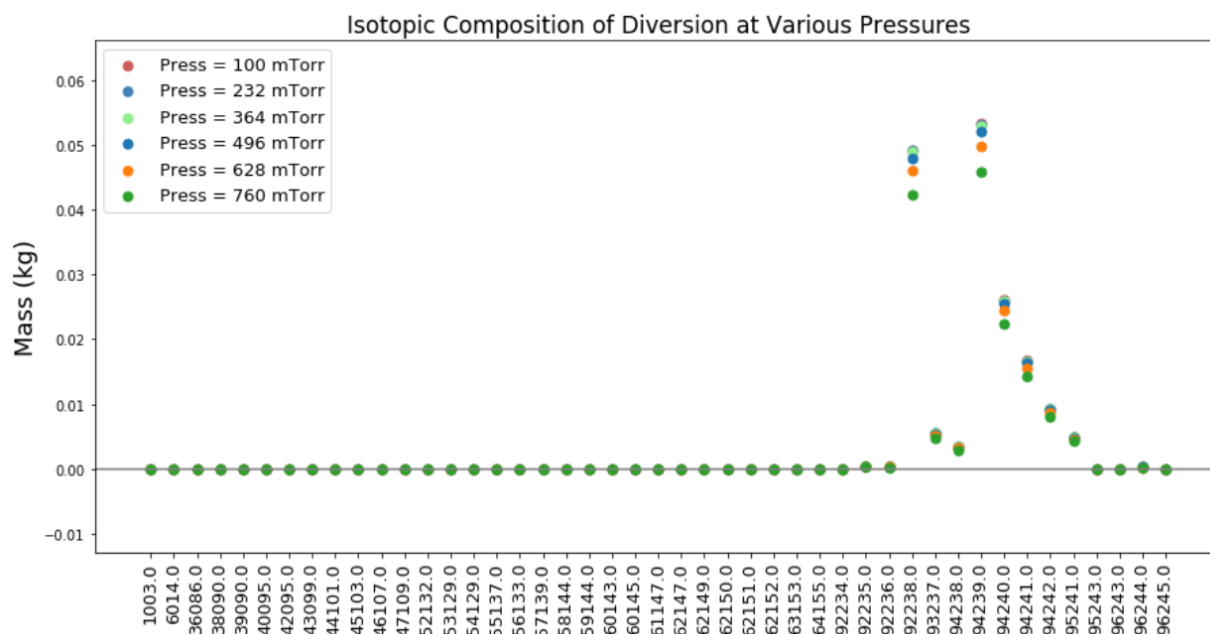
Figure 4.9: Isotopic composition of the Diverted material stream at various Electrowinner currents.

Figure 4.10: Isotopic composition of the Diverted material stream at various Electrowinner flowrates.
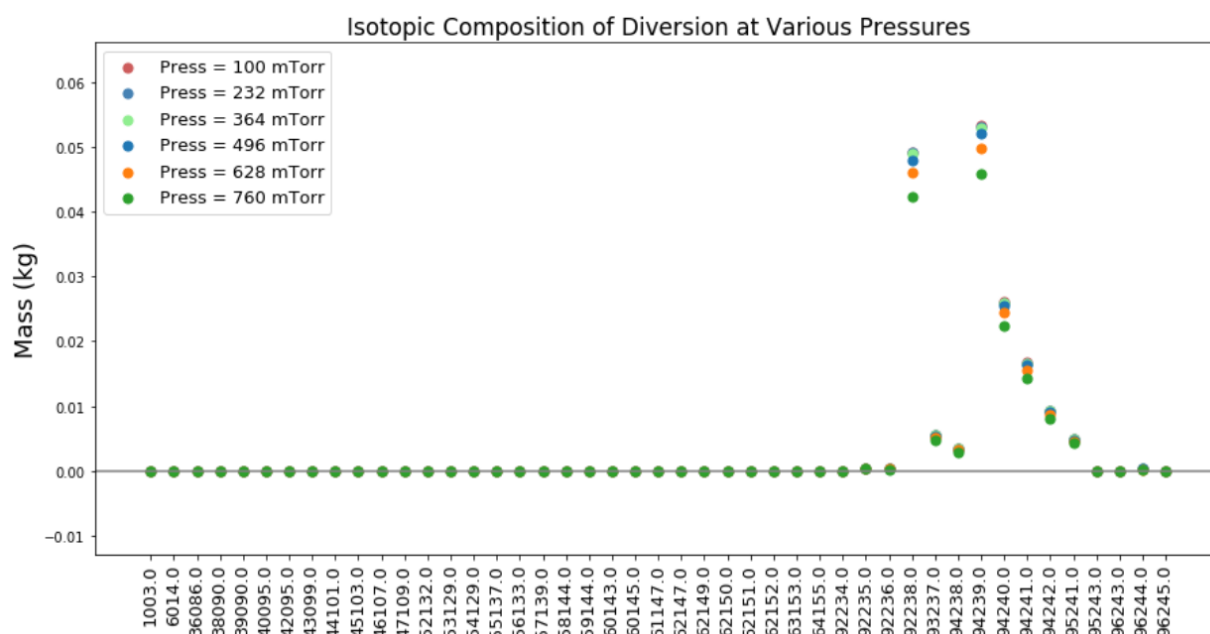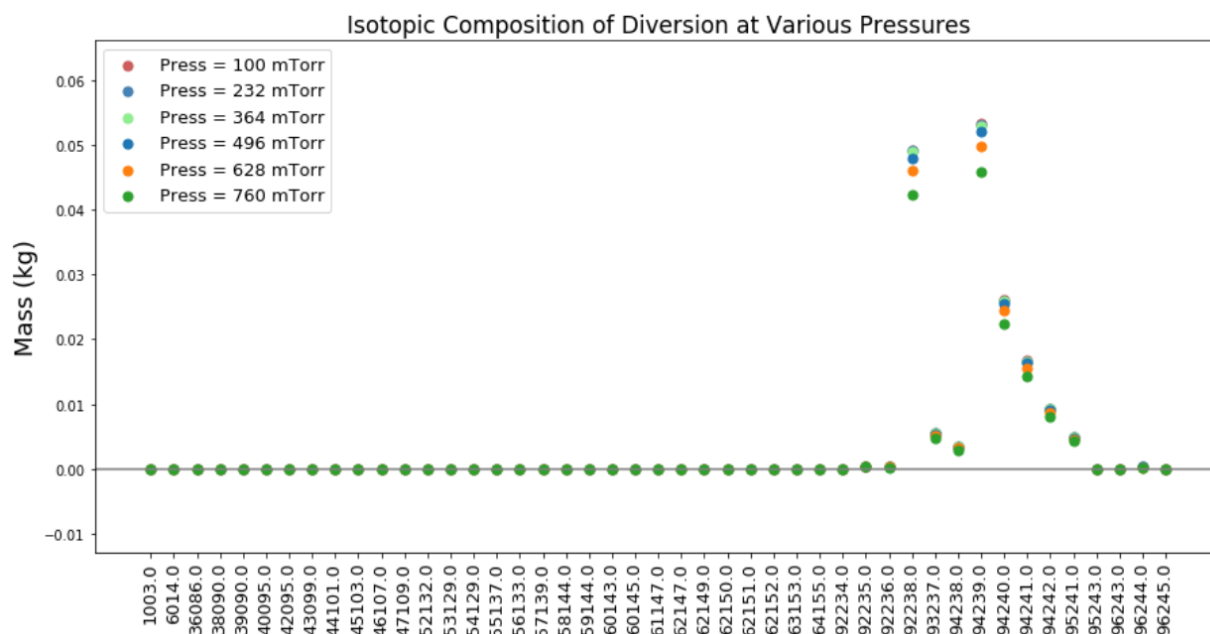
Figure 4.11: Isotopic composition of the Diverted material stream at various Electrowinner flowrates.
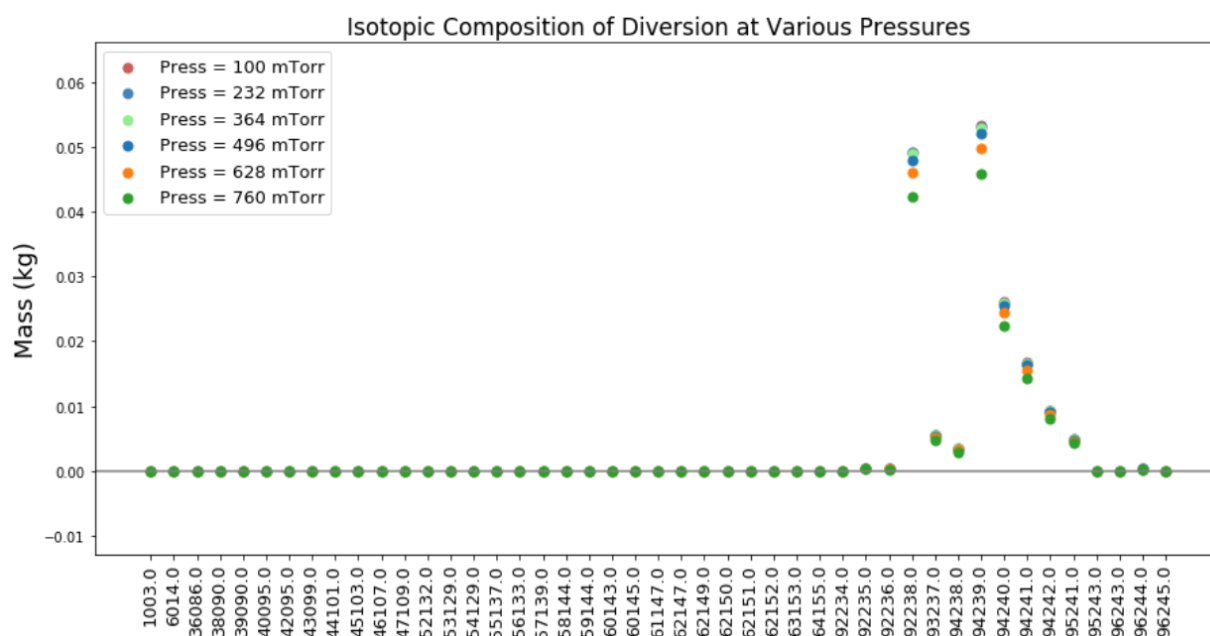

Figure 4.12: Isotopic composition of the Diverted material stream at various Electrowinner reprocessing durations.
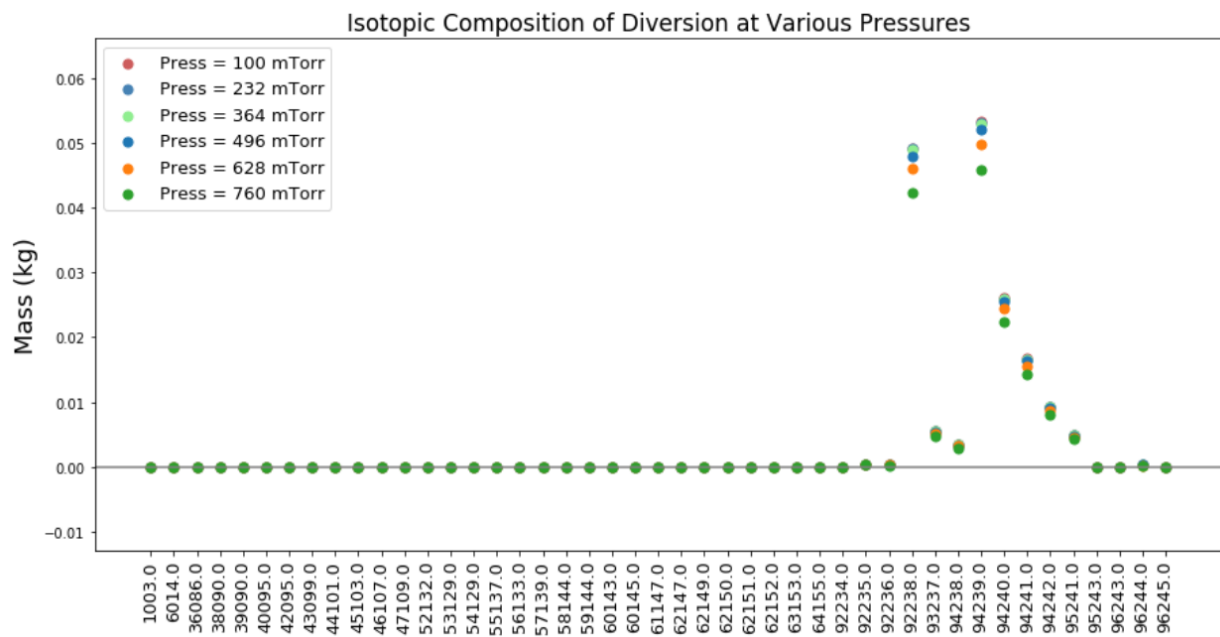
Figure 4.13: Isotopic composition of the Diverted material stream at various Electrowinner reprocessing durations.

Chapter 5

Conclusion

This thesis was motivated by a lack of medium fidelity pyroprocessing plants in current fuel cycle simulators [7]. Combined with the need for safeguards by design in next generation nuclear fuel cycle facilities, a pyroprocessing facility with diversion capabilities fills a technological gap. Pyre brings more detailed separations processes to nuclear fuel cycle simulators informed by more limited and specific electrochemical models such as SSPM and AMPYRE [31].

CYCLUS provides a modular interface to expand and test the capabilities of reprocessing and material diversion. We developed Pyre in the C++ CYCLUS environment to leverage this modular framework and test the facility in a key pyroprocessing transition-scenario. We ran a full US fuel cycle transitioning from LWRs to SFRs using only Pyre facilities to facilitate this transition. We verified Pyre's role in this transition-scenario by observing the simulation's uranium utilization, TRU production, and successful fueling and operation of SFRs to meet power demands.

We also used this transition-scenario to test the

5.1 Future Work

42

References

[1] "Serving Nuclear Non-Proliferation," 2017. [Online]. Available: https://www.iaea.org/sites/default/files/17/12/sg-serving-nuclear-non-proliferation.pdf

[2] K. D. Huff, M. J. Gidden, R. W. Carlsen, R. R. Flanagan, M. B. McGarry, A. C. Opotowsky, E. A. Schneider, A. M. Scopatz, and P. P. H. Wilson, "Fundamental concepts in the Cyclus nuclear fuel cycle simulation framework," *Advances in Engineering Software*, vol. 94, pp. 46–59, Apr. 2016. [Online]. Available: http://www.sciencedirect.com/science/article/pii/S0965997816300229

[3] Michael F. Simpson, "Developments of Spent Nuclear Fuel Pyroprocessing Technology at Idaho National Laboratory," Tech. Rep. INL/EXT-12-25124, 1044209, Mar. 2012. [Online]. Available: http://www.osti.gov/servlets/purl/1044209/

[4] H. Lee, J. H. Lee, S. B. Park, Y. S. Lee, E. H. Kim, and S. W. Park, "Advanced Electrorefining Process at KAERI," *ATALANTE*, May 2008. [Online]. Available: http://www.iaea.org/inis/collection/NCLCollectionStore/_Public/40/032/40032685.pdf

[5] A. A. Frigo, D. R. Wahlquist, and J. L. Willit, "A conceptual advanced pyroprocess recycle facility." Proc., American Nuclear Society : La Grange, IL, pp. 981-985, Tech. Rep. ANL/CMT/CP-111325, Jan. 2003. [Online]. Available: https://www.osti.gov/biblio/981298

[6] I. A. E. Agency, Ed., *Implications of partitioning and transmutation in radioactive waste management*, ser. Technical report series. Vienna: International Atomic Energy Agency, 2004, no. no. 435, oCLC: ocm59136942.

[7] R. A. Borrelli, J. Ahn, and Y. Hwang, "Approaches to a practical systems assessment for safeguardability of advanced nuclear fuel cycles," *Nuclear Technology*, vol. 197, pp. 248–264, Mar. 2017.

[8] R. Wigeland, T. Taiwo, H. Ludewig, M. Todosow, W. Halsey, J. Gehin, R. Jubin, J. Buelt, S. Stockinger, K. Jenni, and B. Oakley, "Nuclear Fuel Cycle Evaluation and Screening - Final Report," *US Department of Energy*, p. 51, 2014. [Online]. Available: https://fuelcycleevaluation.inl.gov/Shared%20Documents/ES%20Main%20Report.pdf

[9] A. C. de Dios, "Introduction to electrochemistry," *GeorgeTown University*.

[10] Organisation for Economic Co-operation and Development, "Spent Nuclear Fuel Reprocessing Flowsheet," *Nuclear Energy Agency*, June 2012. [Online]. Available: https://www.oecd-nea.org/science/docs/2012/nsc-wpfc-doc2012-15.pdf

[11] R. Jubin, "Spent Fuel Reprocessing," Oak Ridge National Lab. (ORNL), Oak Ridge, TN (United States), Tech. Rep., 2009. [Online]. Available: http://www.cresp.org/NuclearChemCourse/monographs/07_Jubin_Introduction%20to%20Nuclear%20Fuel%20Cycle%20Separations%20-%20Final%20rev%202_3_2_09.pdf

[12] H. Ohta, T. Inoue, Y. Sakamura, and K. Kinoshita, "Pyroprocessing of Light Water Reactor Spent Fuels Based on an Electrochemical Reduction Technology," *Nuclear Technology*, vol. 150, no. 2, pp. 153–161, May 2005. [Online]. Available: https://doi.org/10.13182/NT05-A3613

[13] J.-M. Hur, C.-S. Seo, S.-S. Hong, D.-S. Kang, and S.-W. Park, "Electrochemical Reduction of Uranium Oxides in Li2o-LiCl Molten-salt," p. 7.

[14] Y. Sakamura, "Separation of Actinides from Rare Earth Elements by Electrorefining in LiCl-KCl Eutectic Salt," *J. Nucl. Sci. Technol.*, vol. 35, no. 1, pp. 49–59, Jan. 1998.

[15] S. Phongikaroon, "Introduction to Pyroprocessing Technology for Used Nuclear Fuel."

[16] H. Lee, J.-M. Hur, J.-G. Kim, D.-H. Ahn, Y.-Z. Cho, and S.-W. Paek, "Korean Pyrochemical Process R&D activities," *Energy Procedia*, vol. 7, pp. 391–395, 2011. [Online]. Available: http://linkinghub.elsevier.com/retrieve/pii/S1876610211015608

[17] R. W. Carlsen, M. Gidden, K. D. Huff, A. C. Opotowsky, O. Rakhimov, A. M. Scopatz, and P. Wilson, "Cycamore v1.0.0," June 2014.

[18] Organisation for Economic Co-operation and Development, "Spent Nuclear Fuel Reprocessing Flowsheet," *Nuclear Energy Agency*, June 2012. [Online]. Available: https://www.oecd-nea.org/science/docs/2012/nsc-wpfc-doc2012-15.pdf

[19] S. X. Li, T. A. Johnson, B. R. Westphal, K. M. Goff, and R. W. Benedict, "Electrorefining Experience for Pyrochemical Processing of Spent EBR-II Driver Fuel," no. 487, p. 7, 2005.

[20] E.-Y. Choi and S. M. Jeong, "Electrochemical processing of spent nuclear fuels: An overview of oxide reduction in pyroprocessing technology," *Progress in Natural Science: Materials International*, vol. 25, no. 6, pp. 572–582, Dec. 2015. [Online]. Available: http://linkinghub.elsevier.com/retrieve/pii/S1002007115001197

[21] H. Lee, J. H. Lee, S. B. Park, Y. S. Lee, E. H. Kim, and S. W. Park, "Advanced Electrorefining Process at KAERI," *ATALANTE 2008*, May 2008. [Online]. Available: http://www.iaea.org/inis/collection/NCLCollectionStore/_Public/40/032/40032685.pdf

[22] L. Chapman and C. Holcombe, "Revision of the uranium-iron phase diagram," *Journal of Nuclear Materials*, vol. 126, no. 3, pp. 323–326, Nov. 1984. [Online]. Available: http://linkinghub.elsevier.com/retrieve/pii/0022311584900461

[23] T. Koyama, Y. Sakamura, M. Iizuka, T. Kato, T. Murakami, and J.-P. Glatz, "Development of Pyro-processing Fuel Cycle Technology for Closing Actinide Cycle," *Procedia Chemistry*, vol. 7, pp. 772–778, 2012. [Online]. Available: http://linkinghub.elsevier.com/retrieve/pii/S187661961200191X

[24] T.-J. Kim, G.-Y. Kim, D. Yoon, D.-H. Ahn, and S. Paek, "Development of an anode structure consisting of graphite tubes and a SiC shroud for the electrowinning process in molten salt," *Journal of Radioanalytical and Nuclear Chemistry*, vol. 295, no. 3, pp. 1855–1859, Mar. 2013. [Online]. Available: http://link.springer.com/10.1007/s10967-012-2103-5

[25] E. Hou, Y. Yilmaz, and A. O. Hero, "Diversion detection in partially observed nuclear fuel cycle networks," 2016.

[26] Y. Yilmaz, E. Hou, and A. O. Hero, "Online diversion detection in nuclear fuel cycles via multimodal observations," 2016.

[27] H. Lee, H. Suk Im, and G. Il Park, "Modeling of oxide reduction in repeated-batch pyroprocessing," *Annals of Nuclear Energy*, vol. 88, pp. 1–11, Feb. 2016. [Online]. Available: http://linkinghub.elsevier.com/retrieve/pii/S0306454915005174

[28] T.-H. Lee, Y.-S. Kim, T.-J. Kwon, H.-S. Shin, and H.-D. Kim, "Determination of the Plutonium Mass and Curium Ratio of Spent Fuel Assemblies for Input Nuclear Material Accountancy of Pyroprocessing, and Analysis of Their Errors," *Nuclear Technology*, vol. 179, no. 2, pp. 196–204, Aug. 2012. [Online]. Available: https://doi.org/10.13182/NT11-77

[29] "Non-Destructive Assay: Instruments and Techniques for Agency Safeguards," *IAEA Bulletin*, vol. 19, no. 5, pp. 34–37. [Online]. Available: https://www.iaea.org/sites/default/files/publications/magazines/bulletin/bull19-5/19503403437.pdf

[30] B. B. Cipiti, F. A. Duran, B. R. Key, Y. Liu, I. Lozano, and R. Ward, "Modeling and design of integrated safeguards and security for an electrochemical reprocessing facility." Sandia National Laboratories, Tech. Rep. SAND2012-9303, Oct. 2012. [Online]. Available: https://www.osti.gov/biblio/1055891-modeling-design-integrated-safeguards-security-electrochemical-reprocessing-facility

[31] L. E. Maggos, C. Pereira, J. A. F. Caputo, and J. M. Copple, "Update on Electrochemical Mass Balance Modeling for Safeguards," p. 13, 2015.